

Fixed points of nonnegative neural networks

Tomasz J. Piotrowski

TPIOTROWSKI@UMK.PL

*Faculty of Physics, Astronomy and Informatics,
Nicolaus Copernicus University,
Grudziądzka 5/7, 87-100 Toruń, Poland*

Renato L. G. Cavalcante

RENATO.CAVALCANTE@HHI.FRAUNHOFER.DE

*Fraunhofer Heinrich Hertz Institute,
Einsteinufer 37, 10587 Berlin, Germany*

Mateusz Gabor

MATEUSZ.GABOR@PWR.EDU.PL

*Faculty of Electronics, Photonics, and Microsystems,
Wrocław University of Science and Technology,
Wybrzeże Wyspiańskiego 27, 50-370 Wrocław, Poland*

Editor: Aryeh Kontorovich

Abstract

We use fixed point theory to analyze nonnegative neural networks, which we define as neural networks that map nonnegative vectors to nonnegative vectors. We first show that nonnegative neural networks with nonnegative weights and biases can be recognized as monotonic and (weakly) scalable mappings within the framework of nonlinear Perron-Frobenius theory. This fact enables us to provide conditions for the existence of fixed points of nonnegative neural networks having inputs and outputs of the same dimension, and these conditions are weaker than those recently obtained using arguments in convex analysis. Furthermore, we prove that the shape of the fixed point set of nonnegative neural networks with nonnegative weights and biases is an interval, which under mild conditions degenerates to a point. These results are then used to obtain the existence of fixed points of more general nonnegative neural networks. From a practical perspective, our results contribute to the understanding of the behavior of autoencoders, and we also offer valuable mathematical machinery for future developments in deep equilibrium models.

Keywords: Nonnegative neural networks, nonlinear Perron-Frobenius theory, monotonic and (weakly) scalable mappings, fixed point analysis, convergence analysis.

1. Introduction

Neural networks consist of multiple layers that are able to extract patterns of input signals for decision-making without any human intervention. This fact has profound consequences in a wide range of wireless communications, image recognition, and speech processing tasks, where neural networks set high standards of performance LeCun et al. (2015); Goodfellow et al. (2016); Samek et al. (2021). Neural networks have also been recently introduced as efficient iterative regularization methods in inverse problems, which opens a vista of new applications, especially in medical imaging Adler and Öktem (2017); Benning and Burger (2018); Ongie et al. (2020).

Our study is specifically focused on nonnegative neural networks, defined as neural networks that map nonnegative vectors to nonnegative vectors. These networks have been widely used in many applications such as spectral analysis, image processing, and text processing Lemme et al. (2012); Nguyen et al. (2013); Chorowski and Zurada (2015); Hosseini-Asl et al. (2015); Zhou et al. (2016); Ali and Yangyu (2017); Ayinde and Zurada (2018); Su et al. (2018); Chen et al. (2019); Yu et al. (2019); Palsson et al. (2019). Nonnegative networks can be designed to decompose input signals into additive sparse components, leading to the formation of an interpretable hierarchical representation of the input data, mirroring the way the human brain processes sensory inputs Lee and Seung (1999); Shashanka et al. (2008); Lemme et al. (2012); Nguyen et al. (2013); Chorowski and Zurada (2015); Ayinde and Zurada (2018). This principle has been exploited in autoencoders with nonnegative weights, which aims to break down input data into additive features within the encoding layer, which are then additively recombined in the decoding layer to reconstruct the original data Lemme et al. (2012); Ayinde and Zurada (2018). In some scenarios, the gains in transparency and interpretation obtained by restricting the weights of the neural network to be nonnegative do not translate into a significant loss of predictive power Nguyen et al. (2013); Chorowski and Zurada (2015).

Neural networks with nonnegative weights have also been increasingly gaining attention in recent years because of the resurgence of analog neural networks, which have been demonstrated to be both readily implementable and more energy efficient than their digital counterparts Kendall et al. (2020); Paliy et al. (2021). In analog networks, the weight parameters are physically encoded in the conductance of programmable resistors. Thus, these analog neural networks are examples of neural networks that are nonnegative because of the laws of physics. Moreover, various approaches can be used to mitigate the loss of predictive power caused by the physical nonnegative constraints Kendall et al. (2020). These results are consistent with those obtained with the digital neural networks in Nguyen et al. (2013); Chorowski and Zurada (2015).

With the objective of improving our understanding of nonnegative neural networks, we shed light on questions related to the existence of fixed points and the shape of the fixed point set of nonnegative neural networks (with matching input and output spaces). To illustrate the importance of fixed point analysis using concrete examples, let us first consider autoencoders, which can be seen as self-mappings taking the form $T : \mathbb{R}^k \rightarrow \mathbb{R}^k$ with $x \mapsto T_1(T_2(x))$, where $T_1 : \mathbb{R}^k \rightarrow \mathbb{R}^l$ with $k > l$ is a mapping (encoder) used to learn compact representations of typical inputs, and $T_2 : \mathbb{R}^l \rightarrow \mathbb{R}^k$ is a mapping (decoder) used to reconstruct the input from the compact representation obtained with T_1 . From this mathematical perspective, the fixed points of an autoencoder T are exactly the inputs that can be perfectly reconstructed. It is therefore important to determine whether the fixed point set of an autoencoder is nonempty, and, if so, how rich this set is (i.e., determine its shape).

As a second example of the significance of fixed point analysis in neural networks, we mention deep equilibrium (DEQ) models Bai et al. (2019, 2020); Gilton et al. (2021); Huang et al. (2021); Tsuchida and Ong (2023), which have been increasingly gaining attention from the machine learning community in recent years. The core concept of implicit models is that, instead of designing layers explicitly, as usually done, it suffices to define a layer's objective (target) functional equation to hold, without actually specifying how such a layer

should achieve this goal. More precisely, a DEQ layer maps an input $x \in \mathbb{R}^k$ to an output $z^* \in \text{Fix}(g_x) \subset \mathbb{R}^k$, where $g_x : \mathbb{R}^k \rightarrow \mathbb{R}^k$ is an explicit mapping parameterized by x . In the above definition, closed-form expressions for the implicit function $x \mapsto z^* \in \text{Fix}(g_x)$ are not required, and the numerical scheme used to compute the output $z^* \in \text{Fix}(g_x)$ from a given input x is not specified. As a result, to ensure that the implicit function $x \mapsto z^* \in \text{Fix}(g_x)$ is well-defined and independent of the numerical scheme used to compute the output, it is natural to require $\text{Fix}(g_x)$ to be a singleton for every $x \in X$. This fixed point formulation also allows for direct implicit differentiation, which is crucial for the efficiency of training of DEQ models Bai et al. (2019).

Fixed point analysis in neural networks is also important in the context of inverse problems, which are often formulated as optimization problems with the objective of minimizing a cost function $f : \mathbb{R}^k \rightarrow \mathbb{R}$. These problems are typically solved with algorithms that can be interpreted as fixed point iterations of mappings determined by f . For example, to minimize a cost function $f : \mathbb{R}^k \rightarrow \mathbb{R}$, we can use the standard gradient descent method: $x_{n+1} = (Id - \alpha \nabla f)(x_n)$, $n = 0, 1, 2, \dots$. The objective of this algorithm is to locate a point x^* satisfying $\nabla f(x^*) = 0$, which is also a fixed-point of the mapping $(Id - \alpha \nabla f)$, where $Id : \mathbb{R}^k \rightarrow \mathbb{R}^k : x \mapsto x$ is the identity mapping. Many other iterative algorithms for optimization have a similar interpretation: they can be seen as fixed point algorithms based on a particular instance of the Mann iteration Yamada et al. (2011). One potential limitation of this traditional mathematical approach for inverse problems is that the function f is often imperfectly known (e.g., owing to the uncertainty about the noise distribution), so, in machine learning, data is used to train a neural network that is used as the mapping of a Mann iteration. In this approach, known as *loop unrolling*, the number of layers is directly related to the number of fixed point iterations. As a result, these neural networks effectively emulate a fixed-point seeking algorithm.

In light of the above discussion, it is clear that studying the properties of the fixed point set of neural networks is crucial for the development of general theory able to explain their behavior in many applications. To this end, we show that, for nonnegative neural networks with nonnegative weights and biases, one of the tractable paths for establishing the existence and the shape of fixed point sets is the nonlinear Perron-Frobenius (PF) theory Lemmens and Nussbaum (2012), which is used to study monotonic and weakly scalable mappings defined on a cone (e.g., the nonnegative orthant). As shown in this manuscript, nonnegative neural networks with nonnegative weights and biases can be considered as instances of these mappings under mild and natural assumptions, which opens up the possibility for establishing the existence of fixed points of general nonnegative neural networks. In more detail, we organize the discussion of our results as follows:

1. In Section 2 we introduce notation and key concepts.
2. Section 3 contains the key technical contributions of our study:
 - We first show that nonnegative neural networks with nonnegative weights and biases are, under mild assumptions, both monotonic and (weakly) scalable in the sense of Definition 1 introduced later. This result is a major departure from a recent line of research Chen et al. (2019); Combettes and Pesquet (2020a,b)

that has used convex analysis in Hilbert spaces to study the behavior of neural networks.¹

- Using the monotonicity and weak scalability properties of nonnegative neural networks with nonnegative weights and biases, we then proceed to characterize the shape of the fixed point set of these neural networks in the interior of the nonnegative cone \mathbb{R}_+^k . In particular, we prove that the shape of the fixed point set is often an interval, which degenerates to a point if the neural network is not only weakly scalable, but also scalable. We show that these conditions are weaker than those found in some previous studies, which typically use arguments based on the nonexpansivity of activation functions in Hilbert spaces and operator norms of weight operators Combettes and Pesquet (2020a,b).
3. In Section 4, we give conditions that guarantee that general monotonic nonnegative neural networks have at least one fixed point, and we show that the standard fixed point iteration converges to a fixed point.
 4. In Section 5, we provide conditions for the existence of fixed point(s) of general nonnegative neural networks in settings where Brouwer’s fixed point theorem is not directly applicable.
 5. In Section 6, we illustrate the main theoretical results via numerical simulations, where we evaluate the reconstruction performance of various nonnegative autoencoders. We also discuss how the theoretical contributions of this study provide us with a powerful mathematical machinery for designing efficient DEQ models. Results in this direction are already available in Gabor et al. (2024).
 6. In Section 7, we outline and discuss future research directions, which build on both the theoretical and numerical results provided in Sections 3-6.

2. Key concepts

We start by introducing key concepts and definitions pertaining to vectors and mappings on the nonnegative cone \mathbb{R}_+^k . Let $u, v \in \mathbb{R}_+^k$; then, $u \leq v$ denotes the partial ordering induced by the nonnegative cone, i.e., $u \leq v \Leftrightarrow v - u \in \mathbb{R}_+^k$. Similarly, $u < v$ means that $v - u \in \mathbb{R}_+^k$ and $u \neq v$, while $u \ll v$ means that $v - u \in \text{int}(\mathbb{R}_+^k)$, where $\text{int}(\mathbb{R}_+^k)$ denotes the interior of the nonnegative cone \mathbb{R}_+^k .

Definition 1 *A continuous mapping $f: \mathbb{R}_+^s \rightarrow \mathbb{R}^p$ is said to be*

(A₀) *nonnegative if*

$$\forall x \in \mathbb{R}_+^s \quad f(x) \in \mathbb{R}_+^p, \tag{1}$$

1. In the framework of nonlinear PF theory, monotonicity and (weak) scalability have been widely exploited in the context of wireless networks Boche and Schubert (2008); Schubert and Boche (2011); Shindoh (2019, 2020); Cavalcante et al. (2016); Cavalcante and Stańczak (2019); Cavalcante et al. (2019, 2014, 2017); You and Yuan (2020), economic studies Oshime (1992); Woodford (2022), and biological systems Krause (2015), to cite a few fields.

(A₁) monotonic if

$$\forall x, \tilde{x} \in \mathbb{R}_+^s \quad x \leq \tilde{x} \implies f(x) \leq f(\tilde{x}), \quad (2)$$

(A₂) weakly scalable if

$$\forall x \in \mathbb{R}_+^s \quad \forall \rho \geq 1 \quad f(\rho x) \leq \rho f(x), \quad (3)$$

(A₃) scalable if

$$\forall x \in \mathbb{R}_+^s \quad \forall \rho > 1 \quad f(\rho x) \ll \rho f(x). \quad (4)$$

We use the convention that each subscript applied to A refers to one of the above properties, so that, for example:

- continuous and nonnegative mappings are (A₀)-mappings;
- continuous, nonnegative, and monotonic mappings are (A_{0,1})-mappings;
- continuous, nonnegative, monotonic, and weakly scalable mappings are (A_{0,1,2})-mappings; and
- continuous, nonnegative, monotonic, and scalable mappings are (A_{0,1,2,3})-mappings.

The above classes of mappings satisfy the relations $A_{0,1,2,3} \subset A_{0,1,2} \subset A_{0,1} \subset A_0$ by definition. We will also use the class $A_{0,2}$ of continuous, nonnegative, and weakly scalable mappings in conjunction with a stricter than A_1 notion of monotonicity.

Definition 2 An (A₀)-mapping $f: \mathbb{R}_+^s \rightarrow \mathbb{R}_+^p$ is said to be strictly monotonic if

$$\forall x, \tilde{x} \in \mathbb{R}_+^s \quad x < \tilde{x} \implies f(x) < f(\tilde{x}) \quad \text{and} \quad x \ll \tilde{x} \implies f(x) \ll f(\tilde{x}). \quad (5)$$

We now introduce the standard definition of a neural network.

Definition 3 Let $T_i: \mathbb{R}^{k_{i-1}} \rightarrow \mathbb{R}^{k_i}$ of the form $T_i(x_{i-1}) \stackrel{\text{df.}}{=} \sigma_i(W_i x_{i-1} + b_i)$ be the i -th layer of an n -layered feed forward neural network, $i = 1, \dots, n$, where $x_{i-1} \in \mathbb{R}^{k_{i-1}}$ is the input to the layer, $W_i: \mathbb{R}^{k_{i-1}} \rightarrow \mathbb{R}^{k_i}$ is the linear weight operator (matrix), $b_i \in \mathbb{R}^{k_i}$ is the bias, and $\sigma_i: \mathbb{R}^{k_i} \rightarrow \mathbb{R}^{k_i}$ is the activation function. A neural network T is then the composition

$$T \stackrel{\text{df.}}{=} T_n \circ \dots \circ T_1, \quad (6)$$

with the zeroth layer corresponding to the input to the network. Hereafter, we assume that the input and output layers have the same dimension $k \stackrel{\text{df.}}{=} k_0 = k_n$, which enables us to consider traditional recurrent neural networks and autoencoders as particular cases.

We also assume that the layers of a neural network T taking the form in (6) use separable activation functions in the sense defined below.

Definition 4 Let T_i be the i -th layer of a neural network T in (6). An activation function $\sigma_i: \mathbb{R}^{k_i} \rightarrow \mathbb{R}^{k_i}$ for this layer is composed of k_i scalar activation functions $\sigma_{i_j}: \mathbb{R} \rightarrow \mathbb{R}$ ($j = 1, 2, \dots, k_i$), and its operation is defined as

$$\sigma_i(y_i) = \sum_{j=1}^{k_i} (\sigma_{i_j}(y_{i_j}))e_{i_j}, \quad (7)$$

where $y_{i_j} \in \mathbb{R}$ is the j -th coefficient of the vector $y_i \stackrel{\text{df.}}{=} W_i x_{i-1} + b_i \in \mathbb{R}^{k_i}$ and e_{i_j} is the j -th coefficient of the canonical basis of \mathbb{R}^{k_i} for $j = 1, 2, \dots, k_i$. For later reference, we equivalently express a layer T_i with the activation function σ_i in (7) as

$$T_i(x_{i-1}) = \sigma_i(y_i) = \left(\sigma_{i_1}(y_{i_1}), \sigma_{i_2}(y_{i_2}), \dots, \sigma_{i_{k_i}}(y_{i_{k_i}}) \right), \quad (8)$$

where σ_{i_j} are scalar activation functions for $j = 1, 2, \dots, k_i$.

We are now ready to study the set of fixed points of nonnegative neural networks, which are networks that have already been used in the literature and that are increasingly gaining attention because of the new trends in analog computation Nguyen et al. (2013); Lemme et al. (2012); Ayinde and Zurada (2018); Chorowski and Zurada (2015); Hosseini-Asl et al. (2015); Chen et al. (2019); Ali and Yangyu (2017); Palsson et al. (2019); Su et al. (2018); Kendall et al. (2020); Paliy et al. (2021). With the theory we develop in Sections 3 and 4, we can, for example, understand some limitations of autoencoders and gain insights into useful approaches for improving their reconstruction performance.

3. Fixed points of $(A_{0,1,2})$ -neural networks

We begin with the following assumption.

Assumption 5 In Section 3 we assume that, for all layers $i = 1, \dots, n$:

1. the weight matrices W_i and biases b_i have nonnegative coefficients; and
2. the activation functions σ_i are $(A_{0,1,2})$ -mappings.

In Corollary 9 below, we show that Assumption 5 guarantees that the resulting network is an $(A_{0,1,2})$ -neural network, and, in certain cases, even an $(A_{0,1,2,3})$ -neural network. However, we first demonstrate that Assumption 5.2 holds for activation functions constructed with commonly used scalar activation functions, and we show an explicit construction of neural networks satisfying Assumption 5.

3.1 Construction of $(A_{0,1,2})$ -activation functions

Many commonly used scalar activation functions (σ_{i_j} in Definition 4) are continuous and concave in the nonnegative orthant. Therefore, in light of [Lemma 1]Cavalcante and Stańczak (2019), they belong to a proper subclass of $(A_{0,1,2})$ -scalar activation functions. Some of them are listed below.

Remark 6 *The following two lists provide examples of widely-used continuous scalar concave activation functions (with their domains restricted to $\xi \in \mathbb{R}_+$), and, hence, $(A_{0,1,2})$ -scalar activation functions. We divide them into two classes:*

- *functions satisfying $\lim_{\xi \rightarrow \infty} \sigma'(\xi) = 0$, and*
- *functions satisfying $\lim_{\xi \rightarrow \infty} \sigma'(\xi) = 1$.*

(L1) *continuous scalar concave activation functions satisfying $\lim_{\xi \rightarrow \infty} \sigma'(\xi) = 0$:*

- *(sigmoid) $\xi \mapsto \frac{1}{1+\exp(-\xi)}$*
- *(capped ReLU) $\xi \mapsto \min\{\xi, \beta\}, \beta > 0$*
- *(saturated linear) $\xi \mapsto \begin{cases} 1, & \text{if } \xi > 1; \\ \xi, & \text{if } 0 \leq \xi \leq 1 \end{cases}$*
- *(inverse square root unit) $\xi \mapsto \frac{\xi}{\sqrt{1+\xi^2}}$*
- *(arctangent) $\xi \mapsto (2/\pi) \arctan \xi$*
- *(hyperbolic tangent) $\xi \mapsto \tanh \xi$*
- *(inverse hyperbolic sine) $\xi \mapsto \operatorname{arcsinh} \xi$*
- *(Elliot) $\xi \mapsto \frac{\xi}{1+\xi}$*
- *(logarithmic) $\xi \mapsto \log(1 + \xi)$*

(L2) *continuous scalar concave activation function satisfying $\lim_{\xi \rightarrow \infty} \sigma'(\xi) = 1$:*

- *(ReLU, inverse square root linear unit) $\xi \mapsto \xi$*

The above lists are by no means exhaustive. Indeed, a variety of the commonly used scalar activation functions reduce to a certain function from the above two lists if restricted to \mathbb{R}_+ , so we do not list all variations here. For example, various versions of the ReLU (e.g., parameterized, exponential), including the original ReLU listed above, and also the inverse square root linear unit, reduce to the identity mapping on \mathbb{R}_+ .

The following fact enables us to establish scalability and strict monotonicity of activation functions, and it will be useful later in Section 3.2.

Fact 7 *Consider an $(A_{0,1,2})$ -activation function σ_i constructed with continuous scalar concave activation functions listed in Remark 6. Then:*

- *if all scalar activation functions σ_{i_j} are such that $\sigma_{i_j}(0) > 0$ for $j \in \{1, 2, \dots, k_i\}$, then, by (Cavalcante et al., 2016, Proposition 1), σ_i in (7) is an $(A_{0,1,2,3})$ -activation function. Thus, limiting the choice to scalar activation functions from lists (L1)-(L2) in Remark 6, we obtain that σ_i in (7) is an $(A_{0,1,2,3})$ -activation function only if it is constructed with the sigmoid scalar activation function; and*
- *σ_i in (7) is strictly monotonic if it is constructed with scalar activation functions from lists (L1)-(L2) in Remark 6, except for the capped ReLU and the saturated linear scalar activation functions.*

3.2 Construction of $(A_{0,1,2})$ -neural networks

We now prove that the neural networks satisfying Assumption 5 are in the $(A_{0,1,2})$ class. Namely, the following lemma provides simple sufficient conditions to construct such networks.

Lemma 8 *Consider a neural network T of the form in (6), and let $T_i: \mathbb{R}^{k_{i-1}} \rightarrow \mathbb{R}^{k_i}: x_{i-1} \mapsto \sigma_i(W_i x_{i-1} + b_i)$ be its i -th layer. Then:*

1. *if the affine mapping $y_i = W_i x_{i-1} + b_i$ has nonnegative weights W_i and biases b_i , then it is in $(A_{0,1,2})$;*
2. *if the affine mapping $y_i = W_i x_{i-1} + b_i$ has nonnegative weights W_i and positive biases b_i , then it is in $(A_{0,1,2,3})$;*
3. *if the affine mapping $y_i = W_i x_{i-1} + b_i$ is in $(A_{0,1,2})$ and the activation function σ_i is also in $(A_{0,1,2})$, then the layer T_i is in $(A_{0,1,2})$;*
4. *if the affine mapping $y_i = W_i x_{i-1} + b_i$ is in $(A_{0,1,2})$ and the activation function σ_i is in $(A_{0,1,2,3})$, then the layer T_i is in $(A_{0,1,2,3})$;*
5. *if the affine mapping $y_i = W_i x_{i-1} + b_i$ is in $(A_{0,1,2,3})$, and the activation function σ_i is strictly monotonic and is in the class $(A_{0,2})$, then the layer T_i is in $(A_{0,1,2,3})$;*
6. *if all layers T_i for $i = 1, 2, \dots, n$ are in $(A_{0,1,2})$, then T is an $(A_{0,1,2})$ -neural network;*
7. *if T_{i_0} is in $(A_{0,1,2,3})$ for some $1 \leq i_0 \leq n$, T_i are in $(A_{0,1,2})$ for $i = 1, \dots, i_0 - 1$, and T_i are strictly monotonic and are in $(A_{0,2})$ for $i = i_0 + 1, \dots, n$, then T is an $(A_{0,1,2,3})$ -neural network.*

Proof See Appendix C.

Corollary 9 *Suppose that a neural network T with the general structure in (6) satisfies Assumption 5. Then:*

1. *T is an $(A_{0,1,2})$ -neural network;*
2. *if, in addition, the n -th layer T_n has a bias vector b_n such that $b_n \gg 0$, and it uses a strictly monotonic activation function, then T is an $(A_{0,1,2,3})$ -neural network; or*
3. *if, in addition, the n -th layer T_n uses only $(A_{0,1,2,3})$ activation functions (e.g., sigmoid scalar activation functions), then T is an $(A_{0,1,2,3})$ -neural network.*

Proof By Assumption 5 and Lemma 8, points 1 and 3, the layers T_i are in $(A_{0,1,2})$ for $i = 1, \dots, n$. By Lemma 8, point 6, T is an $(A_{0,1,2})$ -neural network, which establishes point 1 above. Furthermore, if the additional assumption of point 2 above is used, from Lemma 8, points 2 and 5, we obtain that the layer T_n is in $(A_{0,1,2,3})$. In Lemma 8, point 7, we set $i_0 = n$ to obtain the assertion of point 2 above. Similarly, if the additional assumption of point 3 above is used, from the first point in Fact 7 we obtain that σ_n is an $(A_{0,1,2,3})$ -activation function. Thus, from Lemma 8, point 4, we conclude that T_n is in $(A_{0,1,2,3})$. For $i_0 = n$, from Lemma 8, point 7, we conclude that T is an $(A_{0,1,2,3})$ -neural network. ■

3.3 Existence and uniqueness of fixed points of $(A_{0,1,2})$ -neural networks

Next, we prove the following key properties of $(A_{0,1,2})$ -neural networks, which, as shown in the previous section, include as a subset neural networks satisfying Assumption 5:

1. We provide conditions for the existence of fixed points of an $(A_{0,1,2})$ -neural network (Corollary 14).
2. We provide conditions for the uniqueness of the fixed point of a neural network T in cases where T is:
 - (a) an $(A_{0,1,2,3})$ -neural network (Corollary 15),
 - (b) a strongly primitive² $(A_{0,1,2})$ -neural network, and with its activation functions constructed with the continuous scalar concave activation functions listed in Remark 6 (Corollary 20).
3. We show that the condition for the existence of a fixed point of an $(A_{0,1,2})$ -neural network (Corollary 14) is weaker than those obtained using arguments in convex analysis (Remark 17).
4. We provide numerically efficient methods for verifying the existence and uniqueness of fixed point(s) of $(A_{0,1,2})$ -neural networks (Proposition 19 and Corollary 20).

3.3.1 NONLINEAR SPECTRAL RADIUS OF AN $(A_{0,1,2})$ -NEURAL NETWORK

The path toward obtaining the main results of Section 3.3 is via the concept of the asymptotic mapping associated with an $(A_{0,1,2})$ -neural network (Definition 10), and we provide a closed algebraic form of the asymptotic mapping of an $(A_{0,1,2})$ -neural network in Proposition 11. This result is then used to determine the (nonlinear) spectral radius of an $(A_{0,1,2})$ -neural network in Corollary 13.

Definition 10 *Let $T : \mathbb{R}_+^k \rightarrow \mathbb{R}_+^k$ be an $(A_{0,1,2})$ -neural network of the form (6). The asymptotic mapping associated with T is the mapping defined by*

$$T_\infty : \mathbb{R}_+^k \rightarrow \mathbb{R}_+^k : x \mapsto \lim_{p \rightarrow \infty} \frac{1}{p} T(px). \quad (9)$$

We recall that the above limit always exists Cavalcante et al. (2019).

We now prove that the asymptotic mapping T_∞ associated with an $(A_{0,1,2})$ -neural network T is linear, even if the activation functions are possibly nonlinear. This property is very special because asymptotic mappings are nonlinear in general Cavalcante et al. (2019), and linearity is a property that can be exploited to simplify the analysis of the set of fixed points of $(A_{0,1,2})$ -neural networks.

For the common case of a nonnegative neural network with activation functions constructed with continuous scalar concave activation functions listed in Remark 6, we have the following result:

2. The definition of strong primitivity is given in Definition 18 below.

Proposition 11 *Consider a neural network T of the form in (6) with nonnegative weight matrices and biases. Assume that the activation functions are constructed with continuous scalar concave activation functions from lists (L1)-(L2) in Remark 6. Then T is an $(A_{0,1,2})$ -neural network. Moreover:*

1. *If all layers use continuous scalar concave activation functions from list (L2) in Remark 6, then the asymptotic mapping of T is given by $T_\infty(x) = \prod_{i=n}^1 W_i x$.*
2. *On the other hand, if at least one layer of T uses only continuous scalar concave activation functions from list (L1) in Remark 6, then $T_\infty(x) = 0$.*

Proof From Remark 6 we obtain that σ_i are $(A_{0,1,2})$ -activation functions for $i = 1, 2, \dots, n$. Thus, T satisfies both parts of Assumption 5, and, hence, from Corollary 9, point 1, we obtain that T is an $(A_{0,1,2})$ -neural network.

Case 1) : Define

$$T_{1,\infty}(x) \stackrel{\text{df.}}{=} \lim_{p \rightarrow \infty} \frac{1}{p} T_1(px) = \lim_{p \rightarrow \infty} \frac{\sigma_1(W_1 px + b_1)}{p}.$$

Applying L'Hôpital's rule to the coordinate continuous scalar concave activation functions $(\sigma_{1,j} : \mathbb{R} \rightarrow \mathbb{R})_{j \in \{1, \dots, k_1\}}$ from list (L2) in Remark 6, with the scalar p as their arguments with x fixed, we deduce

$$T_{1,\infty}(x) = \lim_{p \rightarrow \infty} \sigma_1'(W_1 px + b_1) W_1 x = W_1 x.$$

Analogously, for the second layer we have

$$T_{1,2,\infty}(x) \stackrel{\text{df.}}{=} \lim_{p \rightarrow \infty} \frac{1}{p} T_2(T_1(px)) = \lim_{p \rightarrow \infty} \frac{\sigma_2\left(W_2(\sigma_1(W_1 px + b_1)) + b_2\right)}{p}.$$

Then, applying L'Hôpital's rule to the coordinate functions $(\sigma_{2,j} : \mathbb{R} \rightarrow \mathbb{R})_{j \in \{1, \dots, k_2\}}$ from list (L2) in Remark 6, we obtain

$$T_{1,2,\infty}(x) = \lim_{p \rightarrow \infty} \sigma_2'\left(W_2(\sigma_1(W_1 px + b_1)) + b_2\right) W_2 \sigma_1'(W_1 px + b_1) W_1 x = W_2 W_1 x. \quad (10)$$

Proceeding as above for the remaining layers, we conclude that $T_\infty(x) = \prod_{i=n}^1 W_i x$.

Case 2) : If σ_i is composed only of continuous scalar concave activation functions from list (L1) in Remark 6 for some $1 \leq i \leq n$, then $\lim_{p \rightarrow \infty} \sigma_i'(p) = 0$. In such a case, we obtain $T_\infty(x) = 0$, as can be deduced from the special case $n = 2$ in (10). ■

The asymptotic mapping obtained in Proposition 11 associated with an $(A_{0,1,2})$ -neural network T can be used to define the (nonlinear) spectral radius of T as follows:

Definition 12 *The (nonlinear) spectral radius of an $(A_{0,1,2})$ -neural network T of the form (6) is given by the largest eigenvalue of the corresponding (linear) asymptotic mapping Os-hime (1992); Cavalcante et al. (2019):*

$$\rho(T_\infty) = \max\{\lambda \in \mathbb{R}_+ : \exists x \in \mathbb{R}_+^k \setminus \{0\} \text{ s.t. } T_\infty(x) = \lambda x\} \in \mathbb{R}_+.$$

From Proposition 11 and Definition 12 we obtain the following corollary yielding the desired result of this section.

Corollary 13 *Consider a neural network T of the form (6) with nonnegative weight matrices and biases. Assume that the activation functions are constructed with continuous scalar concave activation functions from lists (L1)-(L2) in Remark 6 [from Proposition 11, T is an $(A_{0,1,2})$ -neural network]. Then the spectral radius of T is given by*

$$\rho(T_\infty) = \max\{\lambda \in \mathbb{R}_+ : \exists x \in \mathbb{R}_+^k \setminus \{0\} \text{ s.t. } \prod_{i=n}^1 W_i x = \lambda x\} \quad (11)$$

if all layers $i = 1, 2, \dots, n$ use continuous scalar concave activation function from list (L2) in Remark 6. On the other hand, if at least one layer of T uses only continuous scalar concave activation functions from list (L1) in Remark 6, then $\rho(T_\infty) = 0$.

3.3.2 CONDITIONS FOR EXISTENCE OF FIXED POINTS OF $(A_{0,1,2})$ -NEURAL NETWORKS

The following corollary of Proposition 38 gives a sufficient condition for $(A_{0,1,2})$ -neural networks to have a nonempty fixed point set.

Corollary 14 *Consider an $(A_{0,1,2})$ -neural network T of the form (6). Assume that $\rho(T_\infty) < 1$. Then, from Proposition 38, we have that $\text{Fix}(T) \neq \emptyset$.*

Furthermore, the following corollary shows that for $(A_{0,1,2,3})$ -neural networks, the assertion of Corollary 14 can be significantly strengthened. More precisely, in this setting the condition $\rho(T_\infty) < 1$ is not only sufficient but also necessary to prove the existence and uniqueness of the fixed point.

Corollary 15 *Consider an $(A_{0,1,2,3})$ -neural network T of the form (6). Then, from Proposition 39, the neural network T has a fixed point if and only if $\rho(T_\infty) < 1$. Furthermore, from Proposition 40 the fixed point is unique, and it is also positive as a consequence of the scalability of T .*

3.3.3 COMPARISON OF THE ASSUMPTIONS IMPLYING THE EXISTENCE OF FIXED POINTS OF $(A_{0,1,2})$ -NEURAL NETWORKS

In this subsection, we emphasize that the results of Proposition 11, Corollary 14, and Corollary 15 yield weaker conditions for the existence of fixed points of $(A_{0,1,2})$ -neural networks than existing conditions based on arguments in convex analysis. To establish this claim, we use the following fact.

Fact 16 *Consider a neural network T of the form (6) with nonnegative weight matrices and biases. Assume that the activation functions are constructed with continuous scalar concave activation functions from lists (L1)-(L2) in Remark 6 [from Proposition 11, T is an $(A_{0,1,2})$ -neural network]. A standard result is that the spectral radius of a matrix, in the conventional*

sense in linear algebra, is the infimum of all matrix operator norms, so the spectral radius $\rho(W)$ of the nonnegative matrix W , given by

$$\mathbb{R}^{k \times k} \ni W \stackrel{\text{df.}}{=} \prod_{i=1}^n W_i,$$

can be equivalently written as $\rho(W) = \inf\{\|W\| : \|\cdot\| \text{ - operator norm of } W\}$. Therefore, if all layers $i = 1, 2, \dots, n$ use continuous scalar concave activation function from list (L2) in Remark 6, from Corollary 13 and arguments in classical Perron-Frobenius theory (Meyer, 2000, p. 670) we obtain that

$$\rho(T_\infty) = \rho(W) \leq \|W\| \leq \prod_{i=1}^n \|W_i\|, \quad (12)$$

where the matrix norm $\|\cdot\|$ in (12) is an arbitrary operator norm. The second inequality follows from the submultiplicativity property of operator norms.

We are now able to provide concrete examples of $(A_{0,1,2})$ -neural networks for which the existence of fixed points can be established using the above results, but not from previous arguments based on convex analysis. We summarize them in the following remark.

Remark 17 *Let T be a neural network of the form in (6) with nonnegative weight matrices and biases. Assume that the activation functions are selected from the continuous scalar concave activation functions in lists (L1)-(L2) in Remark 6 [from Proposition 11, T is an $(A_{0,1,2})$ -neural network]. Then:*

- *From Proposition 11 and Corollary 14, we conclude that if at least one layer of T uses only continuous scalar concave activation functions from list (L1) in Remark 6, then T has a nonempty fixed point set for arbitrary (finite) nonnegative weights. No assumptions on the (operator or other) norms of the weight matrices are necessary to guarantee the existence of fixed points.*
- *From Fact 16, we obtain that, even if all layers $i = 1, 2, \dots, n$ use exclusively continuous scalar concave activation functions from list (L2) in Remark 6, the conditions for the existence of a nonempty fixed point set stated in Corollaries 14 and 15 are weaker than those obtained using arguments in convex analysis Combettes and Pesquet (2020a) [see also the bounds on the Lipschitz constant of a neural network with nonnegative weights in (Combettes and Pesquet, 2020b, Section 5.3)].*

3.3.4 NUMERICALLY EFFICIENT METHODS FOR VERIFYING THE EXISTENCE OF FIXED POINTS OF STRONGLY PRIMITIVE $(A_{0,1,2})$ -NEURAL NETWORKS

We now introduce the concepts of primitivity and strong primitivity of $(A_{0,1,2})$ -neural networks. The former is used in Section 3.4.2,³ and the latter is used in Proposition 19 and Corollary 20 below to obtain numerically efficient methods for verifying the existence and uniqueness of fixed points of neural networks.

3. We present both definitions here because they are closely related.

Definition 18 We say that an $(A_{0,1,2})$ -neural network $T: \mathbb{R}_+^k \rightarrow \mathbb{R}_+^k$ is primitive if

$$\forall x \in \mathbb{R}_+^k \setminus \{0\} \quad \exists m \in \mathbb{N} \text{ s.t. } T^m(x) \gg 0.$$

Similarly, we say that T is strongly primitive if

$$\forall x \in \mathbb{R}_+^k \quad \exists m \in \mathbb{N} \text{ s.t. } T^m(x) \gg 0.$$

Proposition 19 Consider an $(A_{0,1,2})$ -neural network $T: \mathbb{R}_+^k \rightarrow \mathbb{R}_+^k$. In addition, assume that there exists $m \in \mathbb{N}$ such that $T^m(0) \gg 0$. Then each of the following holds:

1. T is strongly primitive.
2. If $\rho(T_\infty) < 1$, then $\emptyset \neq \text{Fix}(T) \subset \text{int}(\mathbb{R}_+^k)$. In contrast, if $\rho(T_\infty) > 1$, then $\text{Fix}(T) = \emptyset$.
3. If $H: \mathbb{R}_+^k \rightarrow \mathbb{R}_+^k: x \mapsto T^m(x)$ is an $(A_{0,1,2,3})$ -neural network and T is as in Proposition 11, then T has a fixed point if and only if $\rho(T_\infty) < 1$. Furthermore, $\text{Fix}(T) = \text{Fix}(H)$, and the fixed point of T is unique and positive.
4. If $H: \mathbb{R}_+^k \rightarrow \mathbb{R}_+^k: x \mapsto T^m(x)$ is an $(A_{0,1,2,3})$ -neural network and T is as in Proposition 11 with $\rho(T_\infty) < 1$, then the sequence $(x_n)_{n \in \mathbb{N}}$ generated via $x_{n+1} = T(x_n)$, with $x_1 \in \mathbb{R}_+^k$ arbitrarily chosen, converges to the unique fixed point of T .

Proof 1) By assumption, $\exists m \in \mathbb{N}$ such that $T^m(0) \gg 0$. Let $x \in \mathbb{R}_+^k$. From the monotonicity of T , one has $\forall n \geq m$ $T^n(x) \geq T^n(0) \gg 0$, and the desired result follows.

2) The first statement is immediate from Corollary 14 and strong primitivity of T . Now, for the sake of contradiction, assume that $\rho(T_\infty) > 1$ and the network has a fixed point denoted by $x \in \text{Fix}(T)$. Part 1) of the proposition shows that $x = T^m(x) \gg 0$, which is a contradiction because (Cavalcante and Stańczak, 2019, Proposition 2) asserts that a monotonic and weakly scalable T with $\rho(T_\infty) > 1$ has no fixed points in $\text{int}(\mathbb{R}_+^k)$.

3) From the definition of H , we verify that $\text{Fix}(T) \subseteq \text{Fix}(H)$, because if x^* is such that $T(x^*) = x^*$, then $H(x^*) = T^m(x^*) = x^*$. By repeating the proof of Proposition 11 for H , we obtain that $H_\infty(x) = W^m(x)$ if and only if $T_\infty(x) = \prod_{i=n}^1 W_i x$, where $W \stackrel{\text{df.}}{=} \prod_{i=n}^1 W_i$, and $H_\infty(x) = 0$ if and only if $T_\infty(x) = 0$. Then, for the first case, the equality $\rho(H_\infty) = (\rho(T_\infty))^m$ is obtained from (Johnson and Bru, 1990, Theorem 1), whereas it is immediate for the second case. Hence, in particular, $\rho(T_\infty) < 1$ if and only if $\rho(H_\infty) < 1$.

Now consider the case $\rho(T_\infty) < 1$. Then, we conclude that the extended neural network H has a unique (positive) fixed point as a consequence of the statement in Corollary 15. Moreover, Part 2) of the proposition guarantees that $\text{Fix}(T) \neq \emptyset$, so we must have $\text{Fix}(H) = \text{Fix}(T)$ because $\text{Fix}(H)$ is a singleton and $\emptyset \neq \text{Fix}(T) \subseteq \text{Fix}(H)$. Similarly, for the case $\rho(T_\infty) \geq 1$, we deduce $\rho(H_\infty) = (\rho(T_\infty))^m \geq 1$, which implies $\text{Fix}(H) = \emptyset$ from the statement of Corollary 15. Therefore, T cannot have a fixed point because $\text{Fix}(T) \subseteq \text{Fix}(H) = \emptyset$, and the proof is complete.

4) Part 3) of the proposition and the assumptions of Part 4) guarantee that T and H have a common unique positive fixed point that we denote by $x^* \in \text{int}(\mathbb{R}_+^k)$. We also note that, as T is monotonic and weakly scalable on $\text{int}(\mathbb{R}_+^k)$, by (Lemmens and Nussbaum, 2012, Lemma

2.1.7) it is nonexpansive in the Thompson metric space $(\text{int}(\mathbb{R}_+^k), d_T)$, see Definition 37. Let $i \in \mathbb{N}$ and let $k \geq im$. Then

$$\forall x \in \mathbb{R}_+^k \quad \forall k \geq im \quad d_T(T^k(x), x^*) = d_T(T^k(x), T^{k-im}(x^*)) \leq d_T(T^{im}(x), x^*),$$

where the last inequality follows from the nonexpansivity of T w.r.t. d_T . We note that for $k \geq im$ if $i \rightarrow \infty$ then $k \rightarrow \infty$. Thus, we obtain that

$$\forall x \in \mathbb{R}_+^k \quad \lim_{k \rightarrow \infty} d_T(T^k(x), x^*) \leq \lim_{i \rightarrow \infty} d_T(T^{im}(x), x^*) = \lim_{i \rightarrow \infty} d_T(H^i(x), x^*) = 0,$$

where the last equality follows from (Cavalcante et al., 2019, Fact 1(iv)). ■

One of the practical implications of Proposition 19 is that we can obtain a simple numerical certificate of uniqueness of the fixed point of a monotonic and weakly scalable nonnegative neural network T with concave activation functions, by simply computing $T^m(0)$ for some sufficiently large m , as formally described below. It is also important to note that in such a case, the network T needs only to be monotonic and weakly scalable to have a unique fixed point if $\rho(T_\infty) < 1$, which is a stronger result than the one given in Corollary 15, which requires scalability of the network.

Corollary 20 *Consider a neural network T of the form (6) with nonnegative weight matrices and biases. Assume that the activation functions are selected from the continuous scalar concave activation functions in lists (L1)-(L2) in Remark 6 [from Proposition 11, T is an $(A_{0,1,2})$ -neural network]. If there exists $m \in \mathbb{N}$ such that $T^m(0) \gg 0$, then T has a fixed point if and only if $\rho(T_\infty) < 1$. Furthermore, the fixed point is unique and positive.*

Proof Let $f_1, f_2: \mathbb{R}_+^{k_1} \rightarrow \mathbb{R}_+$ be nonnegative concave functions and let $t \in (0, 1)$. We note that, by [Lemma 1]Cavalcante and Stańczak (2019), they are $(A_{0,1,2})$ -functions. From concavity of f_1 one has

$$f_1(tx_1 + (1-t)x_2) \geq tf_1(x_1) + (1-t)f_1(x_2).$$

Hence, monotonicity of f_2 implies that

$$f_2[f_1(tx_1 + (1-t)x_2)] \geq f_2[tf_1(x_1) + (1-t)f_1(x_2)].$$

From the concavity of f_2 we deduce

$$f_2[tf_1(x_1) + (1-t)f_1(x_2)] \geq tf_2(f_1(x_1)) + (1-t)f_2(f_1(x_2)).$$

By combining the above two inequalities, we conclude that

$$(f_2 \circ f_1)(tx_1 + (1-t)x_2) \geq t(f_2 \circ f_1)(x_1) + (1-t)(f_2 \circ f_1)(x_2),$$

establishing that $f_2 \circ f_1$ is also a nonnegative concave function. We can use induction to extend the validity of the above arguments to an arbitrary number of nonnegative concave functions. By definition, a mapping $F \stackrel{\text{def}}{=} (f_1 \dots, f_{k_2}): \mathbb{R}_+^{k_1} \rightarrow \mathbb{R}_+^{k_2}$ is said to be nonnegative concave if all coordinate functions $(f_1 \dots, f_{k_2})$ are nonnegative concave functions. Thus, we conclude that the layers of T are nonnegative concave mappings because they are constructed

by composing nonnegative affine mappings with nonnegative concave activation functions. Hence, the neural network T is itself a nonnegative concave mapping as a composition of n nonnegative concave layers. Furthermore, $H : \mathbb{R}_+^k \rightarrow \mathbb{R}_+^k : x \mapsto T^m(x)$ is a nonnegative concave mapping because it is the m -fold composition of T with itself. We also deduce that H is necessarily a positive mapping because, by the monotonicity of T , $\forall x \in \mathbb{R}_+^k$ $H(x) = T^m(x) \geq T^m(0) \gg 0$. Concavity and positivity of H in the nonnegative orthant imply that H is an $(A_{0,1,2,3})$ -neural network (Cavalcante et al., 2016, Proposition 1). Thus, from Proposition 19, point 3, we obtain that T has a fixed point if and only if $\rho(T_\infty) < 1$. Furthermore, this fixed point is unique and positive. ■

3.4 The shape of fixed point sets of $(A_{0,1,2})$ -neural networks

In the previous sections, we provided conditions for the existence and uniqueness of fixed points of $(A_{0,1,2})$ -neural networks under different mild assumptions. However, if the fixed point set is not a singleton, we have not yet established the shape of this set. In the following, we address this limitation of the analysis done so far. In more detail, in this section, we show the following results:

1. First, in Section 3.4.1:
 - (a) in Proposition 22, we show the shape of the fixed point set of a generic $(A_{0,1,2})$ -mapping under the assumption of lower- and upper-primitivity (see Definition 21 below) at its fixed points; and
 - (b) we show that the condition of lower- and upper-primitivity is essential to obtain a meaningful shape of the fixed point set of a generic $(A_{0,1,2})$ -mapping, otherwise the fixed point set of such a mapping can be in principle arbitrary (Examples 1 and 2).
2. Afterwards, in Section 3.4.2, we specialize the results of Section 3.4.1 to the case of $(A_{0,1,2})$ -neural networks. More precisely:
 - (a) we compare the results in Section 3.3.2 and Section 3.4.1 related to the shape of the fixed point set of $(A_{0,1,2})$ -neural networks (Remark 25);
 - (b) we derive a numerically verifiable sufficient condition for an $(A_{0,1,2})$ -neural network to be lower- and upper-primitive at its fixed points (Lemma 26).

3.4.1 NONLINEAR PERRON-FROBENIUS THEORY

The results of this section establish the shape of the fixed point sets of $(A_{0,1,2})$ -mappings $f : \mathbb{R}_+^k \rightarrow \mathbb{R}_+^k$ in the interior of the \mathbb{R}_+^k cone. They are derived using tools from nonlinear Perron-Frobenius theory, and the following definition is required to state the main contributions:

Definition 21 (Lemmens and Nussbaum, 2012, Definition 6.5.2) *Let $f : \text{int}(\mathbb{R}_+^k) \rightarrow \text{int}(\mathbb{R}_+^k)$. We say that f is lower-primitive at $x \in \text{int}(\mathbb{R}_+^k)$ if there exists an open neighbourhood $U \subseteq \text{int}(\mathbb{R}_+^k)$ of x such that for each $y \in U$ with $y < x$ there exists an integer $p_y \geq 1$ with $f^{p_y}(y) \ll f^{p_y}(x)$. Likewise, we say that f is upper-primitive at $x \in \text{int}(\mathbb{R}_+^k)$ if there exists*

an open neighbourhood $U \subseteq \text{int}(\mathbb{R}_+^k)$ of x such that for each $y \in U$ with $x < y$ there exists an integer $p_y \geq 1$ with $f^{p_y}(x) \ll f^{p_y}(y)$.

The following proposition provides the shape of the fixed point set of an $(A_{0,1,2})$ -mapping under the conditions of lower- and upper-primitivity. It extends (Cavalcante and Stańczak, 2019, Proposition 3) to the case $x \in \text{int}(\mathbb{R}_+^k)$, and it can be seen as a corollary of (Lemmens and Nussbaum, 2012, Theorem 6.5.6). For clarity, we provide a proof that quotes parts of the original proof of (Lemmens and Nussbaum, 2012, Theorem 6.5.6).

Proposition 22 (cf. Theorem 6.5.6 in Lemmens and Nussbaum (2012)) *Let us define $f : \text{int}(\mathbb{R}_+^k) \rightarrow \text{int}(\mathbb{R}_+^k)$ to be the restriction of an $(A_{0,1,2})$ -mapping to the positive orthant. Furthermore, let $\text{Fix}(f) \neq \emptyset$ and let f satisfy the conditions of lower- and upper-primitivity at $u \in \text{Fix}(f)$. Let $x \in \text{int}(\mathbb{R}_+^k)$. Then, there exists $\lambda_x > 0$ such that $\lim_{p \rightarrow \infty} f^p(x) = \lambda_x u \in \text{Fix}(f)$. Moreover, define*

$$s_0 \stackrel{\text{df.}}{=} \inf\{\lambda > 0 : \lambda u \in \text{Fix}(f)\},$$

and

$$t_0 \stackrel{\text{df.}}{=} \sup\{\lambda > 0 : \lambda u \in \text{Fix}(f)\}.$$

Then:

$$\begin{aligned} \text{if } s_0 > 0 \text{ and } t_0 < \infty &\Rightarrow \text{Fix}(f) = \{\lambda u : s_0 \leq \lambda \leq t_0\}; \\ \text{if } s_0 = 0 \text{ and } t_0 < \infty &\Rightarrow \text{Fix}(f) = \{\lambda u : 0 < \lambda \leq t_0\}; \\ \text{if } s_0 > 0 \text{ and } t_0 = \infty &\Rightarrow \text{Fix}(f) = \{\lambda u : s_0 \leq \lambda\}; \text{ and} \\ \text{if } s_0 = 0 \text{ and } t_0 = \infty &\Rightarrow \text{Fix}(f) = \{\lambda u : 0 < \lambda\}. \end{aligned} \tag{13}$$

Proof Let $u \in \text{Fix}(f)$ and let $x \in \text{int}(\mathbb{R}_+^k)$. As f is monotonic and weakly scalable on $\text{int}(\mathbb{R}_+^k)$, by (Lemmens and Nussbaum, 2012, Lemma 2.1.7) it is nonexpansive in the Thompson metric space $(\text{int}(\mathbb{R}_+^k), d_T)$ (see Definition 37), which is a complete metric space (Lemmens and Nussbaum, 2012, Proposition 2.5.2). We further note from (Piotrowski and Cavalcante, 2022, Remark 3 and Corollary 1) that $(\text{int}(\mathbb{R}_+^k), d_T)$ is also a proper metric space in the sense that every closed ball in $(\text{int}(\mathbb{R}_+^k), d_T)$ is compact.

Denote the orbit of f at x by $\mathcal{O}(x; f) \stackrel{\text{df.}}{=} \{f^p(x) : p = 0, 1, 2, \dots\}$ with $f^0(x) \stackrel{\text{df.}}{=} x$. Then, the orbit $\mathcal{O}(u; f) = \{u\}$ is bounded, thus, by Całka's Theorem (Lemmens and Nussbaum, 2012, Theorem 3.1.7), $\mathcal{O}(x; f)$ is also bounded in $(\text{int}(\mathbb{R}_+^k), d_T)$. The closure $\overline{\mathcal{O}}(x; f)$ of $\mathcal{O}(x; f)$ consists of $\mathcal{O}(x; f)$ and the bounded set of all limit points of subsequences of $\mathcal{O}(x; f)$. Hence, by (Piotrowski and Cavalcante, 2022, Corollary 1), $\overline{\mathcal{O}}(x; f)$ is compact in $(\text{int}(\mathbb{R}_+^k), d_T)$. Then, from (Lemmens and Nussbaum, 2012, Lemma 3.1.2), one has that $f(\omega(x; f)) = \omega(x; f)$, where $\omega(x; f) \stackrel{\text{df.}}{=} \{y \in \text{int}(\mathbb{R}_+^k) : f^{p_i}(x) \rightarrow y \text{ for some } (p_i)_i \text{ with } p_i \rightarrow \infty\}$, and, consequently, $f^p(\omega(x; f)) = \omega(x; f)$ for any $p \in \mathbb{N}$.

Furthermore, by our assumptions on f , we can apply (Lemmens and Nussbaum, 2012, Lemma 6.5.4) to f and conclude that there are two cases: either there exists $0 < \alpha_x \leq 1$ such that $m(y/u) = \alpha_x$ for all $y \in \omega(x; f)$, or there exists $\beta_x \geq 1$ such that $M(y/u) = \beta_x$ for all $y \in \omega(x; f)$, where $m(y/u) \stackrel{\text{df.}}{=} \sup\{\gamma > 0 : \gamma u \leq y\}$ and $M(y/u) \stackrel{\text{df.}}{=} \inf\{\gamma > 0 : y \leq \gamma u\}$. We note that for $y, u \in \text{int}(\mathbb{R}_+^k)$ one has simply $m(y/u) = \min_{i=1, \dots, k} \{y_i/u_i\}$ and $M(y/u) = \max_{i=1, \dots, k} \{y_i/u_i\}$, see (Lemmens and Nussbaum, 2012, eqs.(2.8),(2.9)).

We now show that, in the first case, $\omega(x; f) = \{\alpha_x u\}$. To obtain a contradiction, we assume that there exists $z \in \omega(x; f)$ with $z \neq \alpha_x u$ such that $m(z/u) = \alpha_x$. Then $z_i \geq \alpha_x u_i$ for $i = 1, \dots, k$, and there exists $i_0 \in \{1, \dots, k\}$ such that $z_{i_0} > \alpha_x u_{i_0}$, hence $\alpha_x u < z$. Since f is upper-primitive at u , there exists $p \in \mathbb{N}$ such that

$$\alpha_x u = \alpha_x f^p(u) \ll \alpha_x f^p(\alpha_x^{-1} z) \leq f^p(z),$$

where the second inequality follows from the weak scalability of f . Consequently, $\alpha_x u \ll f^p(z)$. It follows that $m(f^p(z)/u) = \sup\{\gamma > 0 : \gamma u \leq f^p(z)\} > \alpha_x$, which is impossible, as $f^p(z) \in \omega(x; f)$. In a similar way, it can be shown that, in the second case, $\omega(x; f) = \{\beta_x u\}$. Thus, we have proved that there exists $\lambda_x > 0$ such that $\omega(x; f) = \{\lambda_x u\}$.

Consequently, since $f(\omega(x; f)) = \omega(x; f)$, we have $f(\lambda_x u) = \lambda_x u$, thus $\lambda_x u \in \text{Fix}(f)$. We also note that, if $v \in \text{Fix}(f)$ is such that $v \neq u$, we obtain that $\omega(v; f) = \{v\}$, and thus it must be either $v = \alpha_v u$ or $v = \beta_v u$, where $0 < \alpha_v \leq 1$ and $1 \leq \beta_v$.

Furthermore, as $\alpha_x u \leq u \leq \beta_x u$ for each $x \in \text{int}(\mathbb{R}_+^k)$, from (Lemmens and Nussbaum, 2012, Lemma 6.5.5) we obtain that $\text{Fix}(f)$ is in this case one of the intervals in (13). Moreover, from (Lemmens and Nussbaum, 2012, Lemma 3.1.3) for a periodic point with period 1, one has that

$$\lim_{p \rightarrow \infty} f^p(x) = \lambda_x u \in \text{Fix}(f). \blacksquare$$

The conditions of lower- and upper-primitivity are important, as the following examples demonstrate.

Example 1 Let $f : \text{int}(\mathbb{R}_+^2) \rightarrow \text{int}(\mathbb{R}_+^2)$ be defined as $f(x) = (x_1, \min\{2, x_2\})$ for $x = (x_1, x_2) \in \text{int}(\mathbb{R}_+^2)$. Then f is an $(A_{0,1,2})$ -mapping that is also subadditive, see (Oshime, 1992, Example 2.4). We can check that $\text{Fix}(f) = \text{int}(\mathbb{R}_+) \times (0, 2]$. However, neither of the conditions of lower- and upper-primitivity are satisfied by f on $\text{Fix}(f)$, as the following analysis shows.

Let $u = (u_1, u_2) \in \text{Fix}(f)$, and let $x = (2u_1, u_2)$. Then $x \in \text{Fix}(f)$ and $u < x$ because $x \neq u$ and $x - u = (u_1, 0) \in \mathbb{R}_+^2$. However, for all $p_x \geq 1$, we have $f^{p_x}(u) = u \not\ll f^{k_x}(x) = x$ because $x - u = (u_1, 0) \notin \text{int}(\mathbb{R}_+^2)$. Similarly, if $x = (u_1/2, u_2) \in \text{Fix}(f)$, then $x < u$ because $u \neq x$ and $u - x = (u_1/2, 0) \in \mathbb{R}_+^2$. However, for all $p_x \geq 1$, we have $f^{p_x}(x) = x \not\ll f^{p_x}(u) = u$ because $u - x = (u_1/2, 0) \notin \text{int}(\mathbb{R}_+^2)$.

Example 2 Let $f : \text{int}(\mathbb{R}_+^2) \rightarrow \text{int}(\mathbb{R}_+^2)$ be the Gauss arithmetic-geometric mean given by $f(x) = (\frac{x_1+x_2}{2}, \sqrt{x_1 x_2})$ for $x = (x_1, x_2) \in \text{int}(\mathbb{R}_+^2)$. Then f is an $(A_{0,1,2})$ -mapping, and, for each $x \in \text{int}(\mathbb{R}_+^2)$, there exists $\lambda > 0$ such that $\lim_{p \rightarrow \infty} f^p(x_1, x_2) = (\lambda, \lambda)$ (Lemmens and Nussbaum, 2012, Section 1.4). Indeed, it is clear that $\text{Fix}(f) = \{x \in \text{int}(\mathbb{R}_+^2) \mid x_1 = x_2\}$, and, from the properties of arithmetic and geometric means, we verify that f is both lower- and upper-primitive at each $u \in \text{Fix}(f)$. Hence, let $u = (\lambda, \lambda)$ for some $\lambda > 0$, and let $x \in \text{int}(\mathbb{R}_+^2)$. Then, from Proposition 22 we conclude that there exists $\lambda_x > 0$ such that $\lim_{p \rightarrow \infty} f^p(x) = (\lambda_x \lambda, \lambda_x \lambda)$. It is also seen that, in this case, $\text{Fix}(f) = \{(\gamma, \gamma), \gamma > 0\}$, see (13).

We close this section with the following remarks, which will be useful later in this study.

Remark 23 From the proof of Proposition 22 it is seen that, if f is both lower- and upper-primitive at any $u \in \text{Fix}(f)$, then it satisfies these conditions on the whole $\text{Fix}(f)$.

Remark 24 Every $(A_{0,1,2})$ -mapping $f : \text{int}(\mathbb{R}_+^k) \rightarrow \text{int}(\mathbb{R}_+^k)$ has a continuous extension $f_{\text{ext}} : \mathbb{R}_+^k \rightarrow \mathbb{R}_+^k$ that is also an $(A_{0,1,2})$ -mapping (Burbanks et al., 2003, Theorem 3.10). This fact justifies calling f itself an $(A_{0,1,2})$ -mapping in the sense of Definition 1.

3.4.2 APPLICATIONS TO NEURAL NETWORKS

We now specialize the results derived above to neural networks.

Remark 25 From Corollary 15, we verify that, if a neural network T of the form (6) is in $(A_{0,1,2,3})$, then $\text{Fix}(T)$ is either the empty set or a singleton. Moreover, from Corollary 14 and Proposition 22, we conclude that $\text{Fix}(T)$ remains simple if T is more generally an $(A_{0,1,2})$ -neural network, because in this case $\text{Fix}(T)$ is an interval. This result is obtained in Proposition 22 under the assumption that T grows “fast enough” at its fixed points, i.e., it satisfies the conditions of lower- and upper-primitivity on $\emptyset \neq \text{Fix}(T) \subset \text{int}(\mathbb{R}_+^k)$.

From the above remark, we note that providing an easily verifiable sufficient condition of lower- and upper-primitivity to hold at an arbitrary $u \in \text{Fix}(T)$ is important for obtaining information about the shape of the fixed point set of neural networks. Fortunately, for neural networks that are differentiable at their fixed points, the following sufficient condition exists. We note that, in view of Remark 23, it is sufficient to verify this condition for a particular fixed point $u \in \text{Fix}(T)$ to guarantee that it holds for every other point in $\text{Fix}(T)$.

Lemma 26 Consider an $(A_{0,1,2})$ -neural network $T : \text{int}(\mathbb{R}_+^k) \rightarrow \text{int}(\mathbb{R}_+^k)$ of the form (6) along with its continuous extension (see Remark 24). Let T have a fixed point $u \in \text{int}(\mathbb{R}_+^k)$, and let T be differentiable at $u \in \text{int}(\mathbb{R}_+^k)$. Then T is both lower- and upper-primitive at u if the Jacobian matrix of T evaluated at u is primitive.

Proof Since T is differentiable at $u \in \text{int}(\mathbb{R}_+^k)$, it is Fréchet differentiable at $u \in \text{int}(\mathbb{R}_+^k)$ with $DT_u(v) = J_T(u)v$ for $v \in \mathbb{R}^k$, where $DT_u : \mathbb{R}^k \rightarrow \mathbb{R}^k$ is the Fréchet derivative of T at u , and $J_T(u)$ is the Jacobian matrix of T evaluated at u . Then the assertion of the lemma follows from (Lemmens and Nussbaum, 2012, Lemma 6.5.7) specialized to a Fréchet-differentiable mapping at u . ■

Remark 27 With notation as in Lemma 26, the Jacobian $J_T(x)$ of T evaluated at $x \in \text{int}(\mathbb{R}_+^k)$ is nonnegative owing to the monotonicity of T . Moreover, $J_T(x)$ is primitive in the sense of Definition 18 if and only if $\exists p \in \mathbb{N}$ s.t. $J_T^p(x)$ is positive, i.e., all of its entries are strictly positive.

We close Section 3 by anticipating that, later in Fact 31 in Section 4, we establish convergence of the fixed point iteration of any $(A_{0,1})$ -neural network (and, hence, of any $(A_{0,1,2})$ -neural network) to its fixed point.

4. Fixed points of $(A_{0,1})$ -neural networks

The results of Section 3 provide a largely complete answer to the problem of determining fixed point(s) of $(A_{0,1,2})$ -neural networks satisfying Assumption 5 in Section 3. We now proceed to relax the assumptions imposed on the neural networks studied so far. In particular, we extend the concepts of nonnegativity and monotonicity to mappings defined on the whole space as follows:

Definition 28 A continuous mapping $f: \mathbb{R}^s \rightarrow \mathbb{R}^p$ is said to be

(A₀') globally nonnegative if

$$\forall x \in \mathbb{R}^s \quad f(x) \in \mathbb{R}_+^p, \quad (14)$$

(A₁') globally monotonic if

$$\forall x, \tilde{x} \in \mathbb{R}^s \quad x \leq \tilde{x} \implies f(x) \leq f(\tilde{x}), \quad (15)$$

where $u \leq v \Leftrightarrow v - u \in \mathbb{R}_+^s$ for $u, v \in \mathbb{R}^s$.

We note that, with $\zeta \in \mathbb{R}$, the sigmoid: $\zeta \mapsto \frac{1}{1+\exp(-\zeta)}$ and ReLU: $\zeta \mapsto 0$ for $\zeta < 0$ and $\zeta \mapsto \zeta$ for $\zeta \geq 0$ are activation functions that are in $(A_{0',1'})$.

Below, we replace Assumption 5 with the following assumptions, which, in particular, lift the restriction of nonnegative biases in all layers and enlarge the class of possible activation functions.

Assumption 29 For all layers $i = 1, \dots, n$:

1. The weight matrices W_i have nonnegative coefficients.
2. Let $S \in 2^{\{1, \dots, n\}}$, where $2^{\{1, \dots, n\}}$ denotes the power set of $\{1, \dots, n\}$, be the set of layers with activation functions σ_s that belong to the class $(A_{0',1'})$ (e.g., layers constructed with the ReLU or sigmoid scalar activation functions), where $s \in S$. The biases b_s are allowed to be negative.
3. Define $P \stackrel{\text{df.}}{=} \{1, \dots, n\} \setminus S$. Then, the activation functions σ_p for $p \in P$ are required to be in the class $(A_{0,1})$. The biases b_p are assumed to be nonnegative.

To emphasize that Assumption 29 covers well-known activation functions that have not been considered in our analysis until this moment, we list the following activation functions, which are in $(A_{0,1})$ but not in $(A_{0,1,2})$ for $\xi \in \mathbb{R}_+$:

(L3) scalar $(A_{0,1})$ -activation functions:

- (Mish) $\xi \mapsto \xi \tanh(\log(1 + \exp(\xi)))$
- (Swish) $\xi \mapsto \frac{\xi}{1+\exp(-\xi)}$
- (GELU) $\xi \mapsto \xi \Phi(\xi)$, where $\Phi(\xi) \stackrel{\text{df.}}{=} \mathbb{P}(X \leq \xi)$, $X \sim \mathcal{N}(0, 1)$.

Corollary 30 If a neural network T of the form (6) satisfies Assumption 29, then T is an $(A_{0,1})$ -neural network.

Proof If $S \neq \emptyset$, then nonnegativity of layers T_s for $s \in S$ is implied by the assumption that the activation functions σ_s are nonnegative on the whole \mathbb{R}^{k_s} . To establish monotonicity of T_s for $s \in S$, let $x, \tilde{x} \in \mathbb{R}_+^{k_s-1}$ such that $x \leq \tilde{x}$. Then, by Assumption 29, point 1, $W_s x \leq W_s \tilde{x}$, and by Assumption 29, point 2, $\sigma_s(W_s x + b) \leq \sigma_s(W_s \tilde{x} + b)$ for any $b \in \mathbb{R}^{k_s}$. Similarly, if $P \neq \emptyset$, then T_p for $p \in P$ is an $(A_{0,1})$ -layer from Lemma 8, point 1, followed by

an application of Lemma 41, point 2(a). The fact that T is an $(A_{0,1})$ -neural network now follows by application of Lemma 41, point 2(a), across layers. ■

As the following examples show, we may leverage the results of Section 3 together with Fact 34 from Section 5 below to establish the existence of fixed points of $(A_{0,1})$ -neural networks.

Example 3 *Assume that $T_2: \mathbb{R}_+^k \rightarrow \mathbb{R}_+^k$ satisfies Assumption 29 with $S = \{1, \dots, n\}$ and $P = \emptyset$ and such that the $(A_{0',1'})$ -activation functions σ_s are in $(A_{0,1,2})$ if their domains are restricted to $\mathbb{R}_+^{k_s}$, e.g., composed of ReLU or sigmoid activation functions for $s \in S$. Define $L: \mathbb{R}_+^k \rightarrow \mathbb{R}_+^k$ by replacing the negative biases on layers S with arbitrary nonnegative values. Such an L is an $(A_{0,1,2})$ -neural network by Lemma 8, point 3, followed by Lemma 8, point 6, and we have that $\forall x \in \mathbb{R}_+^k T_2(x) \leq L(x)$. We may now use Corollary 14 and Fact 34 to conclude that, if $\rho(L_\infty) < 1$, then $\text{Fix}(T_2) \neq \emptyset$.*

Example 4 *Assume that $T_2: \mathbb{R}_+^k \rightarrow \mathbb{R}_+^k$ satisfies Assumption 29 with $S = \emptyset$ and $P = \{1, \dots, n\}$. Construct a neural network $L: \mathbb{R}_+^k \rightarrow \mathbb{R}_+^k$ from T_2 by replacing the activation functions in layers P with pointwise upper-bounding $(A_{0,1,2})$ -activation functions, e.g., by replacing the Swish, Mish, or GELU activation functions with the ReLU function. Then, analogously as in the previous example, the neural network L is an $(A_{0,1,2})$ -neural network by Lemma 8, point 3, and Lemma 8, point 6, and such that $\forall x \in \mathbb{R}_+^k T_2(x) \leq L(x)$. We can now use Corollary 14 and Fact 34 to conclude that $\text{Fix}(T_2) \neq \emptyset$ if $\rho(L_\infty) < 1$.*

If T_2 satisfies Assumption 29 with $\emptyset \neq S \subsetneq \{1, \dots, n\}$, then the previous two examples can be combined to obtain a pointwise upper-bounding network L that can be used to infer the existence of fixed points of T_2 if $\rho(L_\infty) < 1$.

We close Section 4 with the following fact yielding convergence of the fixed point iteration of an $(A_{0,1})$ -neural network to its fixed point. This fact is well-known, and it can be obtained, for example, by following the proof of (Cavalcante and Stańczak, 2019, Proposition 3). We remark that, although the statement of (Cavalcante and Stańczak, 2019, Proposition 3) considers mappings in class $(A_{0,1,2})$, the proof uses only the assumptions of continuity and monotonicity of the mappings under consideration.

Fact 31 (Cavalcante and Stańczak (2019)) *Let T be an $(A_{0,1})$ -neural network of the form (6) with $\text{Fix}(T) \neq \emptyset$. Then, there exists $x^* \in \text{Fix}(T)$ such that, for all $y \in \text{Fix}(T)$, we have $x^* \leq y$. Furthermore, this least fixed point x^* is obtained as the limit of the fixed point iteration $x_{n+1} \stackrel{\text{df.}}{=} T(x_n)$ of T with $x_1 = 0$.*

5. Fixed points of (A_0) -neural networks

In Section 5, we further relax the assumptions made so far to include in our analysis neural networks that are only nonnegative. More specifically, we replace Assumption 5 with the following:

Assumption 32 *The final n -th layer of the neural network has an (A'_0) -activation function σ_n . All other layers are only required to be constructed with continuous activation functions.*

We emphasize that Assumption 32 imposes no restrictions on the weight matrices or biases. They can have arbitrary real coefficients in any layer. As an immediate consequence of Assumption 32, we have the following result.

Corollary 33 *If a neural network T of the form (6) satisfies Assumption 32, then T is an (A_0) -neural network.*

We close the analytical derivations of this paper with a simple result establishing the existence of a fixed point of an (A_0) -neural network.

Fact 34 *Let $L: \mathbb{R}_+^k \rightarrow \mathbb{R}_+^k$ be an $(A_{0,1})$ -neural network. Assume that $\text{Fix}(L) \neq \emptyset$. Let $T_2: \mathbb{R}_+^k \rightarrow \mathbb{R}_+^k$ be an (A_0) -neural network such that $\forall x \in \mathbb{R}_+^k$ $T_2(x) \leq L(x)$. Then $\text{Fix}(T_2) \neq \emptyset$.*

Proof Define $F \stackrel{\text{df.}}{=} \{x \in \mathbb{R}_+^k: x \leq x^*\}$, where $x^* \in \text{Fix}(L)$. We note that F is convex and compact in the standard Euclidean metric space. Therefore,

$$\forall x \in F \quad \mathbb{R}_+^k \ni T_2(x) \leq L(x) \leq L(x^*) = x^*, \quad (16)$$

which proves that $T_2(x) \in F$ for all $x \in F$. As a result, $T_2|_F$ is a continuous self-mapping on F , and, by Brouwer’s fixed point theorem, it possesses a fixed point in F . ■

Remark 35 *From Fact 34, we conclude that, in order to establish the existence of fixed points of an (A_0) -neural network T_2 of the form (6), it suffices to upper-bound T_2 by an $(A_{0,1})$ -neural network L , which could be, for example, one satisfying Assumption 29 (see Corollary 30). Then, the existence of fixed points of both T_2 and L can be established by upper-bounding L (for example, with the approaches in Examples 3 and 4) by an $A_{0,1,2}$ -neural network T and by using the results of Section 3.*

Remark 36 *The existence of a fixed point of an (A_0) -neural network can be established using Fact 34, but the fixed point iteration of such a network does not necessarily converge to its fixed point.*

Below, we discuss applications of the analytical results derived in this paper.

6. Applications

6.1 Autoencoders

For all experiments in this section, we trained a two-layered autoencoder with input and output layers of dimension $k = 784$ and hidden layer with $k_1 = 200$ neurons.⁴ The networks were trained for 30 epochs using the ADAM optimization algorithm with a learning rate of 0.005. The batch size was set to 64, and, as a loss function, the mean squared error was chosen. To enforce nonnegativity of the weights and biases, the negative values were clipped to zero after each iteration of the ADAM algorithm. The experiments were performed on both the entire MNIST dataset and a subset containing only the digit “zero,” which we refer to as the ZERO dataset. We considered various constraints on the weights and biases, so, to simplify notation, we use the following acronyms in the text that follows:

4. The source code is available at the following link: https://github.com/mateuszgabor/nn_networks.

- NN denotes an autoencoder with nonnegative weights and nonnegative biases;
- PN denotes an autoencoder with positive weights and nonnegative biases;
- NR denotes an autoencoder with nonnegative weights and real-valued biases; and
- RR denotes an autoencoder with real-valued weights and real-valued biases.

6.1.1 SIGMOID NN

In this setup, the autoencoder T uses the sigmoid activation functions in both layers. Thus, according to Corollary 9, point 3, T is an $(A_{0,1,2,3})$ -neural network. The sigmoid activation function is in the list (L1) in Remark 6, and, hence, from Proposition 11, point 2, and Corollary 13, the spectral radius of T is $\rho(T_\infty) = 0$. Thus, from Corollary 15, T has a unique and positive fixed point. Moreover, it follows from Fact 31 that this fixed point can be computed with the fixed point iteration of T starting at $x_1 = 0$. The fixed points obtained on the MNIST and ZERO datasets are presented in Figure 1.

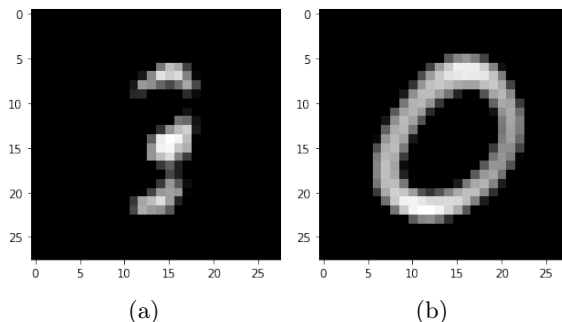


Figure 1: The unique fixed points of an autoencoder with sigmoid activation functions and nonnegative weights and biases on (a) the full MNIST dataset and (b) the ZERO dataset.

6.1.2 TANH NN

In this setup, the autoencoder T uses hyperbolic tangent activation functions in both layers. Thus, according to Corollary 9, point 1, T is an $(A_{0,1,2})$ -neural network. The hyperbolic tangent activation function is in the list (L1) in Remark 6, hence, from Proposition 11, point 2, and Corollary 13, the spectral radius of T is $\rho(T_\infty) = 0$. Thus, from Corollary 14, T has at least one fixed point. Moreover, it follows from Fact 31 that the least fixed point of T can be computed using the fixed point iteration of T starting at $x_1 = 0$. We have also checked that the other fixed points of T can be obtained for different positive starting points of the fixed point iteration of T . However, the sufficient condition of lower- and upper-primitivity of T at its fixed point given in Lemma 26 was not satisfied by T , thus the shape of the fixed point set of T could not be determined. Numerically, the fixed points obtained in the MNIST and ZERO datasets are shown in Figure 2. For the considered case, we have empirical evidence that the shape of the fixed point set is probably an interval, but there is no theory to prove formally this claim at this moment, and this topic should be investigated in future studies.

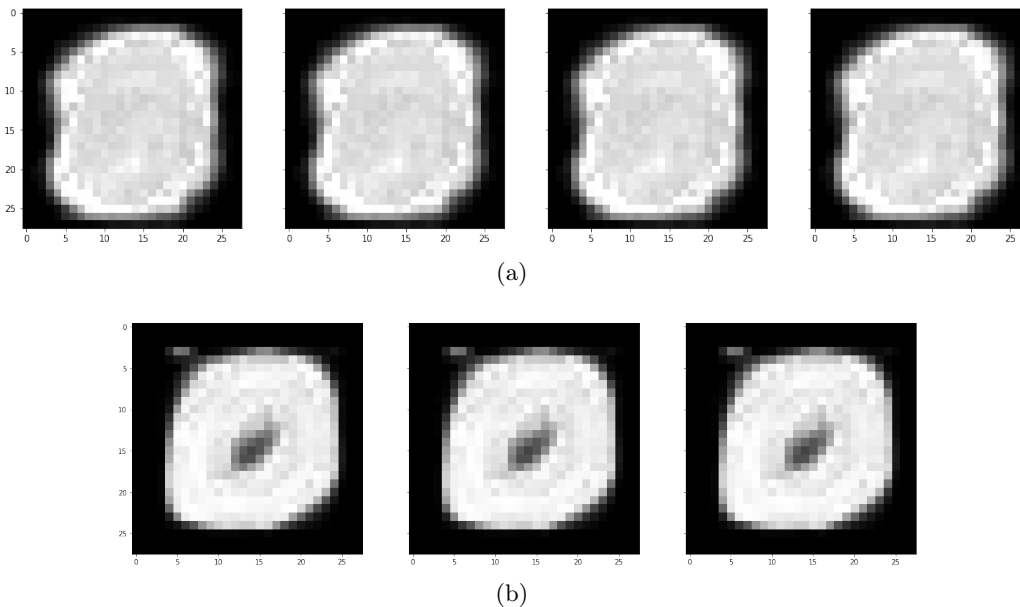


Figure 2: Sample fixed points of an autoencoder with hyperbolic tangent activation functions and with nonnegative weights and biases on (a) the full MNIST dataset and (b) the ZERO dataset.

6.1.3 TANH PN

In this setup, we modified slightly the autoencoder T in Section 6.1.2 by clipping the negative coefficients of the weights in training to 0.001 instead of 0. The resulting autoencoder T has a primitive Jacobian matrix evaluated at a fixed point of T . Hence, by Lemma 26 and Remark 23, such an autoencoder is both lower- and upper-primitive on the whole $\text{Fix}(T)$. Thus, from Proposition 22, we deduce that $\text{Fix}(T)$ is an interval and that the fixed point iteration of T converges to $u \in \text{Fix}(T)$ for any positive starting point $x_1 \gg 0$. Figure 3 depicts fixed points of T obtained for various positive starting points of the fixed point iteration. We note that the fixed points are very similar to the fixed points obtained for the autoencoder in Section 6.1.2.

6.1.4 RELU SPECTRAL NN

In this setup, the autoencoder T used the ReLU activation function in both layers. Thus, according to Corollary 9, point 1, T is an $(A_{0,1,2})$ -neural network. The ReLU activation function is in the list (L2) in Remark 6. Hence, from Proposition 11, point 1, and Corollary 13, the spectral radius of T is $\rho(T_\infty) = \max\{\lambda \in \mathbb{R}_+ : \prod_{i=1}^n W_i x = \lambda x\}$. After training, we obtained a neural network T with $\rho(T_\infty) = 1.01 > 1$ for both the MNIST and ZERO datasets. In such a case, according to (Cavalcante and Stańczak, 2019, Proposition 2), the fixed-point of T may only exist on the boundary of the cone. Indeed, we have numerical evidence that, in this case, the only fixed point of T is the zero vector. Moreover, the obtained autoencoder had a high test loss compared to other setups. Therefore, to obtain a nondegenerate fixed point set of T , we enforced the spectral radius of the autoencoder

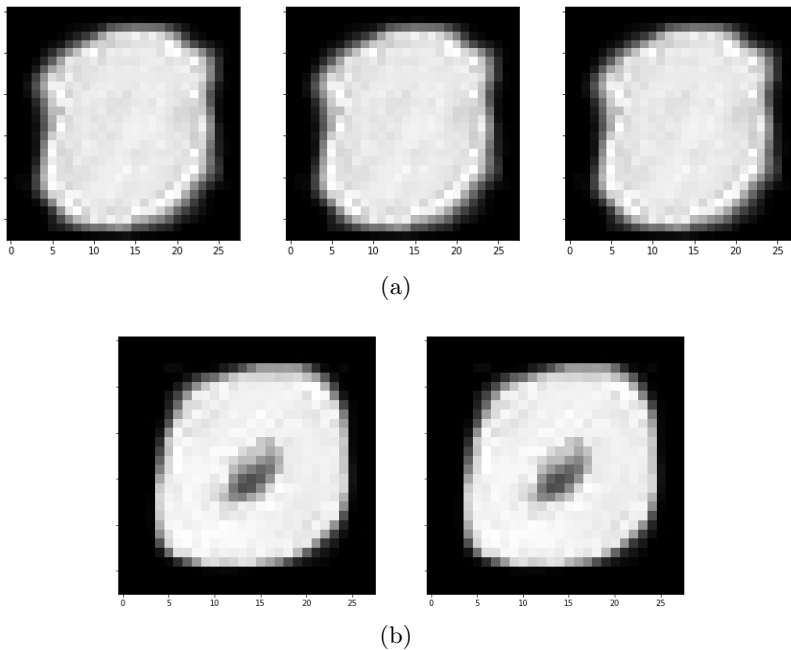


Figure 3: Sample fixed points of an autoencoder with a primitive Jacobian, positive weights, nonnegative biases, and hyperbolic tangent activation functions on (a) the full MNIST dataset and (b) the ZERO dataset.

to be less than 1 using spectral normalization Miyato et al. (2018), which normalizes all weight values by the largest singular value of the weight matrix. Indeed, the spectral radius obtained by the autoencoder T trained with spectral normalization on the MNIST dataset is $\rho(T_\infty) = 0.93$, and, on the ZERO dataset, we have $\rho(T_\infty) = 0.91$. Thus, from Corollary 14, T has at least one fixed point. Moreover, it follows from Fact 31 that the least fixed point of T can be computed with the fixed point iteration of T starting at $x_1 = 0$. We have also checked that the other fixed points of T can be obtained for different positive starting points of the fixed point iteration of T . However, similarly to the Tanh NN autoencoder in Section 6.1.2 above, the sufficient condition of lower- and upper-primitivity of T at its fixed point given in Lemma 26 was not satisfied by T , thus the shape of the fixed point set of T could not be determined. Numerically, the fixed points obtained in the MNIST and ZERO datasets are shown in Figure 4. For this case under consideration, the shape of the fixed point set is probably an interval, but, as already mentioned, at this moment there is no theory to prove formally this claim.

6.1.5 RELU SPECTRAL PN

In this setup, we modified slightly the autoencoder T in Section 6.1.4 by clipping the negative coefficients of the weights during training to 0.001 instead of 0. The resulting autoencoder T has a primitive Jacobian matrix evaluated at a fixed point of T . Hence, by Lemma 26 and Remark 23, such an autoencoder is both lower- and upper-primitive on the whole $\text{Fix}(T)$. Thus, from Proposition 22, we conclude that $\text{Fix}(T)$ is an interval and that the fixed point

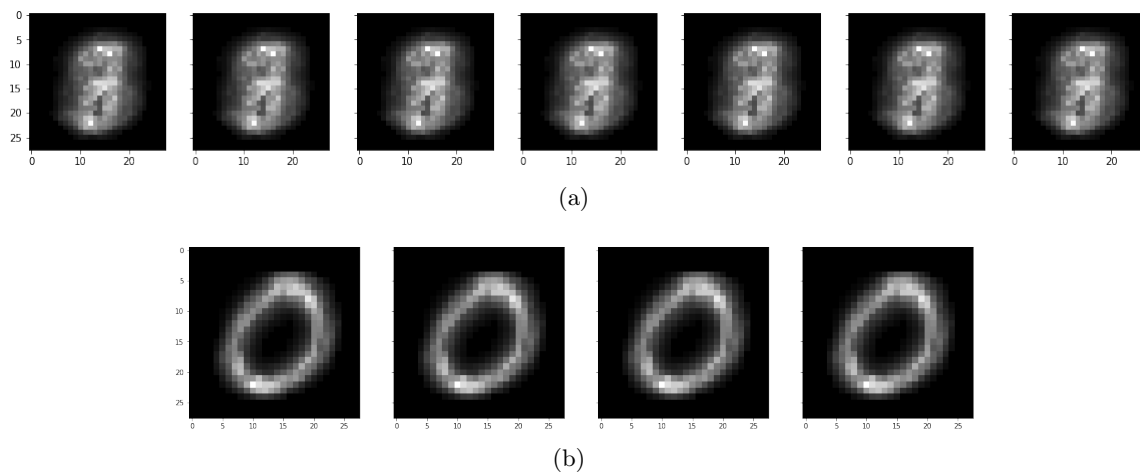


Figure 4: Sample fixed points of an autoencoder with nonnegative weights and biases and with ReLU activation functions using spectral normalization on (a) the MNIST dataset and (b) the ZERO dataset.

iteration of T converges to some $u \in \text{Fix}(T)$ for any positive starting point $x_1 \gg 0$. Figure 5 presents sample fixed points of T obtained for various positive starting points of the fixed point iteration.

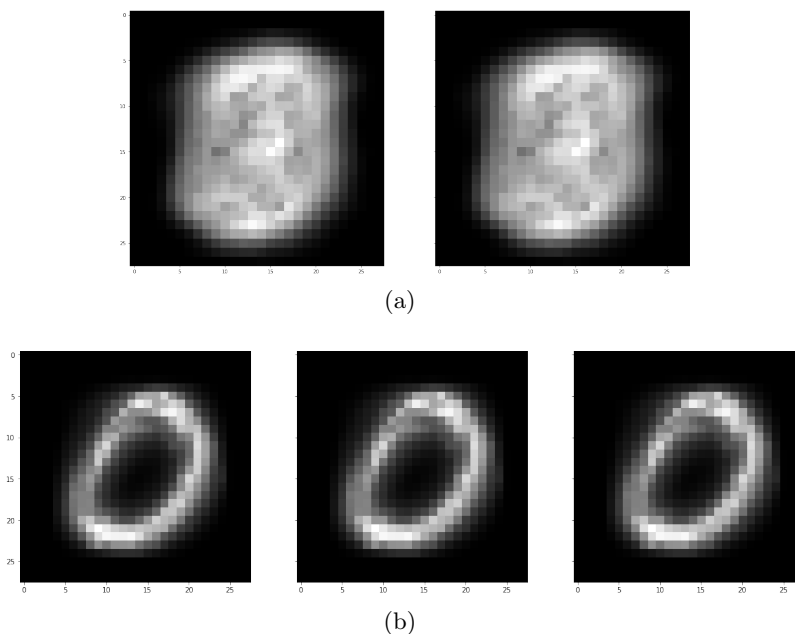


Figure 5: Sample fixed points of an autoencoder with primitive Jacobian, positive weights, nonnegative biases, and ReLU activation functions on (a) the MNIST dataset and (b) the ZERO dataset.

6.1.6 TANH + SWISH NN

In this setup, the autoencoder T_2 used the hyperbolic tangent activation functions in the first layer and the Swish activation functions in the second layer. Such an autoencoder satisfies Assumption 29 for $S = \emptyset$ and $P = \{1, 2\}$, and thus it is an $(A_{0,1})$ -neural network by Corollary 30. Then, following Example 4, this autoencoder is pointwise upper-bounded by an autoencoder L constructed by replacing the Swish activation functions with the ReLU activation functions in the second layer, and we verify that L is an $(A_{0,1,2})$ -neural network. Therefore, using Proposition 11, point 2, and Corollary 13, we obtain that $\rho(L_\infty) = 0$, and, consequently, from Corollary 14 we know that $\text{Fix}(L) \neq \emptyset$. Hence, from Fact 34, we conclude that the autoencoder T_2 has at least one fixed point, and, from Fact 31, we obtain that the least fixed point of T_2 is the limit of the sequence constructed via the fixed point iteration of T_2 starting at $x_1 = 0$. We have also checked that the other fixed points of T_2 can be obtained for different positive starting points of the fixed point iteration of T_2 . The sample fixed points obtained for T_2 are depicted in Figure 6.

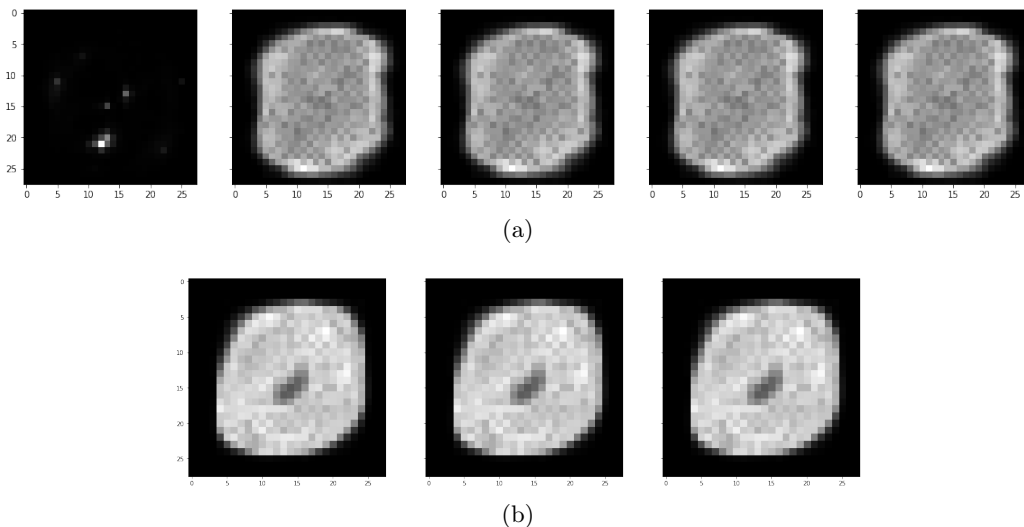


Figure 6: Sample fixed points of an autoencoder with nonnegative weights and biases and with the hyperbolic tangent and Swish activation functions on (a) the MNIST dataset and (b) the ZERO dataset.

6.1.7 RELU + SIGMOID NR

In this setup, the autoencoder T_2 had nonnegative weights and real-valued biases, and it used ReLU activation functions in the first layer and sigmoid activation functions in the second layer. Such an autoencoder satisfies Assumption 29 for $S = \{1, 2\}$ and $P = \emptyset$, and thus it is an $(A_{0,1})$ -neural network by Corollary 30. Then, following Example 3, such an autoencoder is pointwise upper-bounded by the autoencoder L with the same structure but with negative biases replaced with zeros. By doing so, L is an $(A_{0,1,2})$ -neural network. Therefore, using Proposition 11, point 2, and Corollary 13, we verify that $\rho(L_\infty) = 0$. Consequently, from Corollary 14 we deduce that $\text{Fix}(L) \neq \emptyset$. Hence, from Fact 34 we

conclude that the autoencoder T_2 has at least one fixed point, and, from Fact 31, we know that the least fixed point of T_2 can be computed using the fixed point iteration of T_2 starting at $x_1 = 0$. We have also checked that the other fixed points of T_2 can be computed for different positive starting points of the fixed point iteration of T_2 . The sample fixed points obtained for T_2 are depicted in Figure 7.

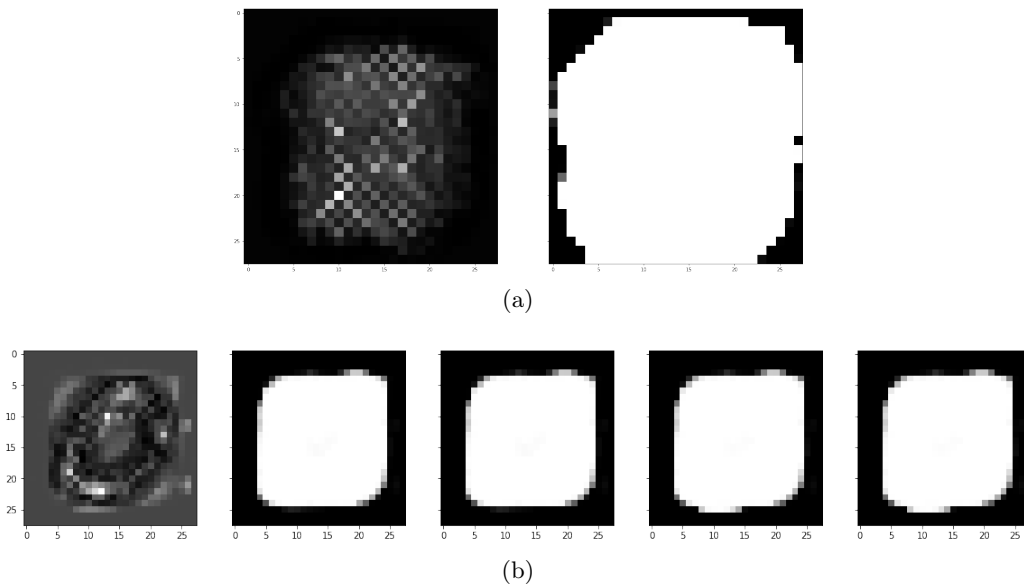


Figure 7: Sample fixed points of an autoencoder with only nonnegative weights and with the ReLU and sigmoid activation functions on (a) the MNIST dataset and (b) the ZERO dataset.

6.1.8 RELU + SIGMOID RR

In this setup, the autoencoder T_2 had real-valued weights and biases, and it used ReLU activation functions in the first layer and sigmoid activation functions in the second layer. Thus, the autoencoder satisfies Assumption 32, and, hence, by Corollary 33, T_2 is an (A_0) -neural network. By replacing negative weights and biases with zeros, we obtain from Corollary 9, point 3, an $(A_{0,1,2,3})$ -neural network L that upper-bounds T_2 . From Proposition 11, point 2, and Corollary 13, we have that $\rho(L_\infty) = 0$, and, from Corollary 15, we conclude that L has a unique and positive fixed point. We note that L is in particular an $(A_{0,1})$ -neural network, which follows from the relations $(A_{0,1,2,3}) \subset (A_{0,1,2}) \subset (A_{0,1})$. Therefore, using Fact 34 and Remark 35, we conclude that $\text{Fix}(T_2) \neq \emptyset$. However, as stated in Remark 36, the fixed point iteration of T_2 does not necessarily converge to its fixed point. Indeed, using the fixed point iteration of T_2 for various starting points, we obtained fixed points for the MNIST dataset, but not for the ZERO dataset. The sample fixed points obtained on the MNIST dataset are depicted in Figure 8.

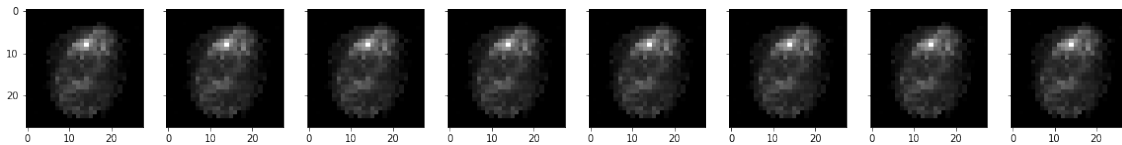


Figure 8: The sample fixed points of an autoencoder with real-valued weights and biases on the MNIST dataset.

Table 1: Empirical mean of the test loss for different configurations of the autoencoders. The test loss is averaged over 10 runs of the autoencoder training. The deviations shown in the table indicate the standard error of the mean, extending one standard error above and below the empirical mean.

Configuration	Test loss
Sigmoid NN 6.1.1	$0.2308 \pm 2.3 \cdot 10^{-6}$
Tanh NN 6.1.2	$0.0063 \pm 3.9 \cdot 10^{-6}$
Tanh PN 6.1.3	$0.0246 \pm 5.6 \cdot 10^{-5}$
ReLU spectral NN 6.1.4	$0.0061 \pm 1.1 \cdot 10^{-5}$
ReLU spectral PN 6.1.5	$0.0059 \pm 1.3 \cdot 10^{-5}$
Tanh + Swish NN 6.1.6	$0.0041 \pm 2.5 \cdot 10^{-6}$
ReLU + Sigmoid NR 6.1.7	$0.0031 \pm 4.7 \cdot 10^{-5}$
ReLU + Sigmoid RR 6.1.8	$0.0042 \pm 7.7 \cdot 10^{-5}$

Table 2: Empirical mean for the spectral radii, products of spectral norms of weight matrices, and spectral norms of product of weight matrices for different configurations of autoencoders. The deviations shown in the table indicate the standard error of the mean, extending one standard error above and below the empirical mean. All values have been computed by considering 10 runs of the autoencoder training.

Configuration	$\rho(T_\infty)$	$\ W_1\ \cdot \ W_2\ $	$\ W_2 \cdot W_1\ $
Sigmoid NN 6.1.1	0.00	6.26 ± 0.07	5.23 ± 0.03
Tanh NN 6.1.2	0.00	373.9 ± 3.8	95.2 ± 0.6
Tanh PN 6.1.3	0.00	35.5 ± 0.6	31.9 ± 0.5
ReLU spectral NN 6.1.4	$0.988 \pm 3.7 \cdot 10^{-4}$	$1.066 \pm 4.7 \cdot 10^{-4}$	$0.999 \pm 4.3 \cdot 10^{-4}$
ReLU spectral PN 6.1.5	$0.987 \pm 7.7 \cdot 10^{-5}$	$1.001 \pm 3.5 \cdot 10^{-5}$	$0.999 \pm 2.9 \cdot 10^{-5}$
Tanh + Swish NN 6.1.6	—	15.8 ± 0.09	8.96 ± 0.04
ReLU + Sigmoid NR 6.1.7	—	123.3 ± 0.7	100.7 ± 0.6
ReLU + Sigmoid RR 6.1.8	—	271.5 ± 0.1	214.7 ± 1.0

6.1.9 CONNECTIONS BETWEEN THE EXISTENCE OF FIXED POINTS, THE NONLINEAR SPECTRAL RADIUS, AND THE SPECTRAL NORM OF THE WEIGHT MATRICES

The fixed points obtained in the above simulations on the MNIST dataset resemble a noisy average of input classes, which is visually very different from any reasonable input signal (i.e., handwritten digits from 0 to 9). In scenarios of this type, fast convergence of the autoencoder

iterations to the set of fixed points is undesirable because the output of the autoencoder can be seen as the first iteration of a fixed point algorithm. Fast convergence of the autoencoders leads to significant differences between the autoencoder input (the handwritten digits) and the output. To optimize the performance of nonnegative autoencoders, a natural strategy is to ensure slow convergence to fixed points for samples of the expected input classes. We discuss this promising but challenging research line in more detail in Section 7.1.1. However, to provide precise mathematical statements that motivate this discussion, we need a clear understanding of some key properties: the nonlinear spectral radius and the weight matrices of the trained neural networks. To this end, we show in Table 1 the performance of the autoencoders considered in this section, and in Table 2 we show key characteristics of these autoencoders with respect to spectral norms of weight matrices and the nonlinear spectral radius. The important aspect to highlight is that previous studies deriving sufficient conditions for the existence of fixed points (and convergence of the fixed point iteration to the fixed points) would require the spectral norm of the product of weight matrices to be strictly less than one, which is a condition often violated in the experiments depicted in Table 2. However, we have verified numerically the existence of fixed points regardless of the values taken by these weight matrices, and these numerical results are consistent with the theory discussed in, for example, Section 3.3.2. We have also verified that, for the autoencoders for which the concept of nonlinear spectral radius is well defined, the best performing autoencoders have spectral radius close to one. This aspect will be crucial for the discussion later in Section 7.1.1.

6.2 Deep equilibrium models

As discussed in the Introduction, fixed point analysis plays a pivotal role in the development of deep equilibrium models. In these models, we typically need to guarantee existence and uniqueness of the fixed point, in addition to establishing convergence of the fixed point iteration. In our recent study in Gabor et al. (2024), we leverage the theoretical framework laid out in the preceding sections to achieve these objectives. More specifically, in that study, we use the results related to $(A_{0,1,2,3})$ -mappings to construct a deep equilibrium model that is guaranteed to have a unique fixed point. Furthermore, we also establish geometric convergence of fixed point iteration based on the results in Piotrowski and Cavalcante (2022). We refer readers to Gabor et al. (2024) for details.

7. Future research directions

Current studies indicate that obtaining simple and general results about the shape of the fixed point set of generic $(A_{0,1})$ -neural networks can be difficult. As an example, a very recent result Reich and Zaslavski (2023) shows that, even for the simple case of (A_1) (continuous and monotonic) self-mappings defined on an interval $[a, b]$, i.e., nondecreasing functions $f: [a, b] \rightarrow [a, b]$, the problem of determining explicitly $\text{Fix}(f)$ is a highly non-trivial task. In particular, (Reich and Zaslavski, 2023, Theorem 2.2) asserts that, for any integer $n \geq 2$, there exists an open and everywhere dense set of such functions for which the cardinality of $\text{Fix}(f)$ is lower bounded by n . Furthermore, any uniqueness conditions on fixed points of $(A_{0,1,2})$ -mappings, beyond those presented in this paper, must clearly preclude simple

cases such as the identity mapping $Id: \mathbb{R}_+^k \rightarrow \mathbb{R}_+^k$, which is the simplest example of an $(A_{0,1,2})$ -mapping with an uncountable number of fixed points ($\text{Fix}(Id) = \mathbb{R}_+^k$).

Two additional important questions, especially from an application perspective, are the following:

- (i) determine the sets of approximate fixed points, that is, find $x \in \mathbb{R}_+^k$ such that $T(x) \approx x$ (in some sense), where T is the nonnegative neural network under consideration; and
- (ii) lift the restriction of nonnegative inputs and outputs.

Below we discuss potential research directions toward these goals.

7.1 Approximate fixed points

At first glance, the imposition of a nonnegativity constraint on neural networks, as explored in this study and inspired by biological mechanisms, might seem to significantly impair their performance. We might expect, for instance, that this constraint could dramatically hinder the ability of neural networks to reconstruct input data perfectly. Nevertheless, we argue that achieving perfect signal reconstruction is unnecessary for a wide array of applications. To support this viewpoint, we refer to the analogy of human cognition, where the brain is understood to process sensory information to a level considered “adequate,” rather than aiming for “perfection.” This viewpoint is consistent with established computational neuroscience principles Doya et al. (2007); Arbib and Bonaiuto (2016); Poggio and Anselmi (2016).

Using this analogy, we posit that autoencoders subjected to nonnegativity constraints can, with proper training, process input data “sufficiently well” in some applications of practical interest. This assertion is supported by empirical evidence Lemme et al. (2012); Ayinde and Zurada (2018), and our discussions in previous sections link this practical aspect with theoretical insights using simple autoencoders on the MNIST dataset. In particular, as briefly mentioned in Section 6.1.9, viewing the output of an autoencoder as the first iteration of a fixed point algorithm offers a natural strategy for developing autoencoders that closely emulate an ideal encoder-decoder model, which compresses and reconstructs perfectly input signals. The nuances of this strategy are explored in the next two subsections.

7.1.1 SLOW CONVERGENCE TO FIXED POINTS

Let us consider the input-output relation $x \mapsto T(x)$ of a nonnegative autoencoder T as the first iteration of the fixed point algorithm $x_{n+1} \stackrel{\text{df.}}{=} T^n(x)$ for $n \in \mathbb{N}$. From this fixed point theory viewpoint, an autoencoder T is expected to provide good reconstruction performance ($x \approx T(x)$) if the fixed point algorithm $x_{n+1} = T^n(x)$ generates slowly converging or diverging sequences. Building on the theoretical foundations laid out in prior sections, we now introduce simple, analytically justified heuristics designed to fulfill this objective.

For the special case of a positive concave autoencoder T ,⁵ which belongs to the subclass of $(A_{0,1,2,3})$ -autoencoders, the results in (Piotrowski and Cavalcante, 2022, Remark 8) and

5. For example, autoencoders T of the form (6) that satisfies $T(0) \gg 0$ and that uses activation functions constructed with continuous scalar concave activation functions from lists (L1)-(L2) in Remark 6. The Sigmoid NN autoencoder considered in Section 6.1.1 is an example of a positive concave neural network. See also Corollary 20.

(Cavalcante and Stańczak, 2018, Proposition 5) derive a contraction factor $c \in [0, 1)$ that indicates the rate of geometric convergence of the fixed point iteration of T to its unique fixed point in Euclidean spaces. The closer c is to one, the slower the convergence speed of the fixed point algorithm is expected to be, and, hence, the better reconstruction performance we may expect from the autoencoder. While a contraction factor c close to the value one does not provide us with formal guarantees of small progress at the first iteration, we illustrate via a simple numerical experiment that designing autoencoders experiencing potentially slow convergence or divergence in their fixed point iterations is a useful strategy to enhance their performance.

In more detail, for positive concave autoencoders, the contraction factor c is lower bounded by the spectral radius $\rho(T_\infty)$, and $\rho(T_\infty) < 1$ if and only if the autoencoder is c -Lipschitz continuous with $c < 1$ in a neighborhood of the fixed point with respect to Thompson’s metric described in Definition 37 in the Appendix Piotrowski and Cavalcante (2022). If $\rho(T_\infty) > 0$, it follows from (11) that we can modify the autoencoder T to have its spectral radius to an arbitrary nonnegative value u by simply rescaling the weights of any layer by $u/\rho(T_\infty)$, so, based on the above arguments, we should set u to a value close to one to improve the performance of autoencoders. This idea is similar to spectral normalization of neural network layers, but our motivation for normalization is uniquely grounded in fixed point theory, providing further theoretical justifications even in nonlinear settings. To demonstrate that this principle can also be exploited by autoencoders that are not necessarily positive and concave, we conducted an experiment with the trained $(A_{0,1,2})$ -ReLU spectral PN autoencoder T from Section 6.1.5. We rescaled the weights of the first layer of T to obtain 25 instances of the autoencoder T with spectral radii $[0.92, 0.93, 0.94, \dots, 1.2]$. The results are shown in Figure 9, and we verify that the test loss indeed achieves its minimum value if the spectral radius is close to one. More precisely, if $1 - \epsilon < c < 1$ for some sufficiently small $\epsilon > 0$, we may expect slowly converging fixed point iterations. On the other hand, if $1 \leq c < 1 + \epsilon$, Figure 9 suggests that autoencoders with slowly diverging fixed point iterations are also able to produce good approximate fixed points.

The above considerations constitute only a sample starting point of a much deeper analysis that is necessary to establish approximate fixed points of more general nonnegative neural networks. As another example of a possible direction towards this goal, we note that, for the ReLU spectral PN autoencoder considered above, if W_1W_2 is diagonalizable and the input classes are (approximately) within the subspace spanned by the eigenvectors of W_1W_2 corresponding to eigenvalues approximately equal to one, we should observe the “slow-convergence” behaviour described above, and, consequently, good reconstruction performance of the autoencoder.

7.1.2 LIPSCHITZ CONTINUITY IN NORMED VECTOR SPACES

Many of the networks we have considered in the previous sections are in fact c -Lipschitz continuous with $c \leq 1$ with respect to Thompson’s metric defined in the Appendix. However, we now show that, in normed vector spaces – which are arguably the spaces of most practical significance for engineers – providing bounds on the Lipschitz constant is not likely to succeed because the best Lipschitz constant can be prohibitively large in Euclidean settings. This insight provides us with information about the output variability in response to minor input

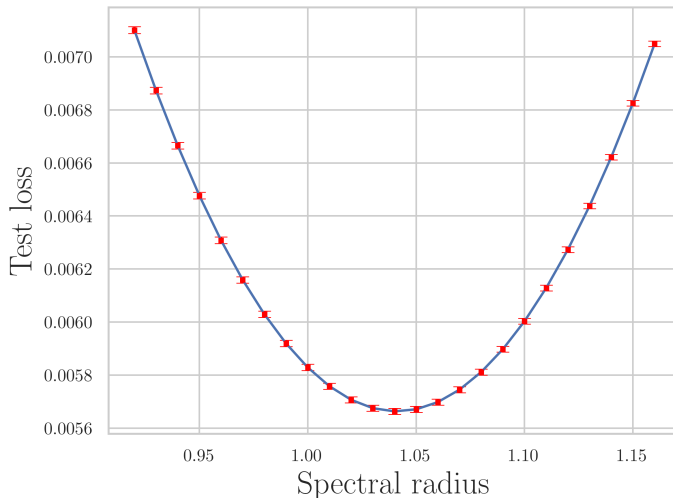


Figure 9: Empirical mean of the test loss as a function of the spectral radius for the ReLU spectral PN autoencoder described in Section 6.1.5 on the MNIST dataset. The test loss is averaged over 10 runs of the autoencoder training. The error bars indicate the standard error of the mean, extending one standard error above and below the empirical mean.

modifications in Euclidean settings. Importantly, it also provides us with a means of evaluating the robustness of neural networks against adversarial attacks.

More precisely, the result in (Combettes and Pesquet, 2020a, Section 2) shows that all activation functions from lists (L1)-(L2) in Remark 6 are nonexpansive in a Hilbert space. Thus, from (Combettes and Pesquet, 2020b, Proposition 4.3), we deduce that neural networks satisfying the conditions in Definitions 3-4, and, in particular, those considered in Sections 3-5, are Lipschitz continuous, and the corresponding Lipschitz constant θ in the standard Euclidean space can be bounded by the spectral norm $\|\cdot\|$ of the weight matrices W_1, \dots, W_n , or, more precisely:

$$\left\| \prod_{i=n}^1 W_i \right\| \leq \theta \leq \prod_{i=1}^n \|W_i\|. \quad (17)$$

The results presented in Table 2 at the end of Section 6.1 show that, for $n = 2$, the lower bound of the spectral norm $\left\| \prod_{i=n}^1 W_i \right\|$ (achievable by neural networks with nonnegative weights (Combettes and Pesquet, 2020b, Section 5.3)) is too large to obtain meaningful bounds for $\|T(x) - x\|$ around its fixed point(s) $x^* \in \text{Fix}(T)$, where the vector norm $\|\cdot\|$ is the standard Euclidean norm. Therefore, a more subtle argument, perhaps based on local Lipschitz continuity for specific input classes, should be considered for exploiting the continuity of T with the aim of determining all inputs x satisfying $T(x) \approx x$, or, equivalently, $\|T(x) - x\| \approx 0$.

7.2 Extending the current results beyond nonnegativity

This study mostly focuses on monotonic neural networks with nonnegative inputs and outputs, but a well-known pre- and post-processing step enables us to extend the above results

to a particular class of monotonic neural networks with inputs and outputs possibly taking values in the whole real line. More precisely, let $T : \text{int}(\mathbb{R}_+^k) \rightarrow \text{int}(\mathbb{R}_+^k)$ be a neural network with a structure that can be analyzed with the theory in this study. To train and operate a neural network of this type with inputs and outputs taking values in \mathbb{R}^k , we can proceed as follows. Let $L : \text{int}(\mathbb{R}_+^k) \rightarrow \mathbb{R}^k : x \mapsto [\log(x_1), \dots, \log(x_k)]$ and $E : \mathbb{R}^k \rightarrow \text{int}(\mathbb{R}_+^k) : x \mapsto [\exp(x_1), \dots, \exp(x_k)]$ denote, respectively, the coordinate-wise log and exponential mappings. Now, consider the neural network defined by $N : \mathbb{R}^k \rightarrow \mathbb{R}^k : x \mapsto L(T(E(x)))$; i.e., we first map an input in \mathbb{R}^k to $\text{int}(\mathbb{R}_+^k)$ with the exponential mapping, process the mapped input with the original positive neural network T , and then map the output of T back to \mathbb{R}^k with the log mapping. Some properties of N can be directly deduced from T . For example, we verify that N has a fixed point if and only if T also has a fixed point. Furthermore, the uniqueness of the fixed point of T implies the uniqueness of the fixed point of N . These are all properties that can be verified with the theory described in the previous sections. From a mathematical perspective, the mapping L is the known isometry between Thompson’s metric space $(\text{int}(\mathbb{R}_+^k), d_T)$ (see Definition 37) and the normed vector space $(\mathbb{R}^k, \|\cdot\|_\infty)$, and further properties of the neural network N are strongly connected to the theory of topical mappings (Lemmens and Nussbaum, 2012, Sect. 1.5).

8. Conclusion

We have shown that the behavior of many neural networks that can be seen as self-mappings with nonnegative weights (as often proposed in the literature) can be rigorously analyzed with the framework of nonlinear Perron-Frobenius theory. We also demonstrated that the concept of the spectral radius of asymptotic mappings is useful for determining whether a neural network has an empty or nonempty fixed point set, and, for an autoencoder, we recall that its fixed point set corresponds to the inputs that can be perfectly reconstructed at the output. Our conditions for the existence of fixed points of nonnegative neural networks are weaker than those previously considered in the literature, which are often based on arguments in convex analysis in Hilbert spaces.

Acknowledgments

The authors are grateful to anonymous reviewers for their constructive comments which surely promoted the readability of the revised manuscript. This work was in part supported by the National Centre for Research and Development of Poland (NCBR) under grant EIG CONCERT-JAPAN/04/2021 and by the Federal Ministry of Education and Research of Germany under grant 01DR21009 and the programme “Souverän. Digital. Vernetzt.” Joint project 6G-RIC, project identification numbers: 16KISK020K and 16KISK030.

Appendix A. Known results

Definition 37 *We define Thompson’s metric by*

$$\begin{aligned} d_T : \text{int}(\mathbb{R}_+^k) \times \text{int}(\mathbb{R}_+^k) &\rightarrow [0, \infty) \\ (x, y) &\mapsto \ln(\max\{M(x, y), M(y, x)\}), \end{aligned} \tag{18}$$

where

$$\begin{aligned} M : \text{int}(\mathbb{R}_+^k) \times \text{int}(\mathbb{R}_+^k) &\rightarrow [0, \infty) \\ (x, y) &\mapsto \inf\{\beta > 0 \mid x \leq \beta y\}. \end{aligned}$$

We call the metric space $(\text{int}(\mathbb{R}_+^k), d_T)$ the *Thompson metric space*.

Proposition 38 ((Cavalcante and Stańczyk, 2019, Proposition 1)) *Let $T: \mathbb{R}_+^k \rightarrow \mathbb{R}_+^k$ be an $(A_{0,1,2})$ -mapping. If $\rho(T_\infty) < 1$, then $\text{Fix}(T) \neq \emptyset$.*

Proposition 39 ((Cavalcante et al., 2019, Proposition 4)) *Let $T: \mathbb{R}_+^k \rightarrow \text{int}(\mathbb{R}_+^k)$ be an $(A_{0,1,2,3})$ -mapping. Then $\text{Fix}(T) \neq \emptyset$ if and only if $\rho(T_\infty) < 1$.*

Proposition 40 ((Cavalcante et al., 2019, Fact 1(ii))) *Let $T: \mathbb{R}_+^k \rightarrow \mathbb{R}_+^k$ be an $(A_{0,1,2,3})$ -mapping. Then $\text{Fix}(T) \neq \emptyset$ is either a singleton or the empty set.*

Appendix B. Construction of monotonic and weakly scalable mappings

The following general lemma introduces building blocks to construct $(A_{0,1,2})$ -mappings, or even $(A_{0,1,2,3})$ -mappings. It extends (Oshime, 1992, Proposition 2.3) to mappings that are not necessarily self-mappings.

Lemma 41

1. Let $f_1: \mathbb{R}_+^s \rightarrow \mathbb{R}_+^p$ and $f_2: \mathbb{R}_+^s \rightarrow \mathbb{R}_+^p$ be (A_0) -mappings and let $\alpha, \beta \geq 0$. Consider the following mappings:

$$x \mapsto (\alpha f_1 + \beta f_2)(x), \tag{19}$$

$$x \mapsto \max\{f_1(x), f_2(x)\}, \tag{20}$$

$$x \mapsto \min\{f_1(x), f_2(x)\}. \tag{21}$$

Then we have:

- (a) If f_1, f_2 are $(A_{0,1})$ -mappings, then so are the mappings in (19)-(21).
 - (b) If f_1, f_2 are $(A_{0,1,2})$ -mappings, then so are the mappings in (19)-(21).
 - (c) If f_1 is an $(A_{0,1,2})$ -mapping and f_2 is an $(A_{0,1,2,3})$ -mapping, $\alpha \geq 0$ and $\beta > 0$, then the mapping in (19) is an $(A_{0,1,2,3})$ -mapping.
 - (d) If f_1, f_2 are $(A_{0,1,2,3})$ -mappings, then so are the mappings in (20)-(21).
2. Let $g: \mathbb{R}_+^p \rightarrow \mathbb{R}_+^r$ be an (A_0) -mapping and consider the following mapping:

$$x \mapsto (g \circ f_1)(x). \tag{22}$$

- (a) If f_1, g are $(A_{0,1})$ -mappings, then so is the mapping in (22).
- (b) If f_1, g are strictly monotonic, then so is the mapping in (22).
- (c) If f_1 is an $(A_{0,2})$ -mapping and g is an $(A_{0,1,2})$ -mapping, then the mapping in (22) is an $(A_{0,2})$ -mapping.

- (d) If f_1 is an $(A_{0,2})$ -mapping and g is an $(A_{0,1,2,3})$ -mapping, then the mapping in (22) is an $(A_{0,2,3})$ -mapping.
- (e) If f_1 is an $(A_{0,2,3})$ -mapping, and g is a strictly monotonic $(A_{0,2})$ -mapping, then the mapping in (22) is an $(A_{0,2,3})$ -mapping.

Proof

Part 1: Properties of mappings in (19)-(21)

1.(a) Let $x, \tilde{x} \in \mathbb{R}_+^s$ be such that $x \leq \tilde{x}$, let $\alpha, \beta \geq 0$, and let f_1, f_2 be $(A_{0,1})$ -mappings. Then $\alpha f_1(x) \leq \alpha f_1(\tilde{x})$ and $\beta f_2(x) \leq \beta f_2(\tilde{x})$. By adding these two inequalities we obtain monotonicity of $x \mapsto (\alpha f_1 + \beta f_2)(x)$. Furthermore, we also have $\max\{f_1(x), f_2(x)\} \leq \max\{f_1(\tilde{x}), f_2(\tilde{x})\}$ and $\min\{f_1(x), f_2(x)\} \leq \min\{f_1(\tilde{x}), f_2(\tilde{x})\}$.

1.(b) Let $x \in \mathbb{R}_+^s$, let $\alpha, \beta \geq 0$, and let f_1, f_2 be $(A_{0,1,2})$ -mappings. Fix $\rho \geq 1$. Then $\alpha f_1(\rho x) \leq \alpha \rho f_1(x)$ and $\beta f_2(\rho x) \leq \beta \rho f_2(x)$. By adding these two inequalities we obtain weak scalability of $x \mapsto (\alpha f_1 + \beta f_2)(x)$. Furthermore, we have $\max\{f_1(\rho x), f_2(\rho x)\} \leq \max\{\rho f_1(x), \rho f_2(x)\} = \rho \max\{f_1(x), f_2(x)\}$, with the same arguments for weak scalability of $\min\{f_1(\rho x), f_2(\rho x)\}$.

1.(c) Let f_1 be an $(A_{0,1,2})$ -mapping and f_2 be an $(A_{0,1,2,3})$ -mapping, with $\alpha \geq 0$ and $\beta > 0$, and let $\rho > 1$. Then $\alpha f_1(\rho x) \leq \alpha \rho f_1(x)$ and $\beta f_2(\rho x) \ll \beta \rho f_2(x)$. By adding these two inequalities we obtain scalability of $x \mapsto (\alpha f_1 + \beta f_2)(x)$.

1.(d) We have $\max\{f_1(\rho x), f_2(\rho x)\} \ll \max\{\rho f_1(x), \rho f_2(x)\} = \rho \max\{f_1(x), f_2(x)\}$, with the same arguments for scalability of $\min\{f_1(\rho x), f_2(\rho x)\}$.

Part 2: Properties of mapping in (22)

2.(a) Let $x, \tilde{x} \in \mathbb{R}_+^s$ be such that $x \leq \tilde{x}$ and let f_1, g be $(A_{0,1})$ -mappings. Then $f_1(x) \leq f_1(\tilde{x})$, and, hence, $g(f_1(x)) \leq g(f_1(\tilde{x}))$.

2.(b) As above.

2.(c) Let $x \in \mathbb{R}_+^s$, and let f_1 be an $(A_{0,2})$ -mapping and g be an $(A_{0,1,2})$ -mapping. Fix $\rho \geq 1$. From weak scalability of f_1 , we have $f_1(\rho x) \leq \rho f_1(x)$, and, from monotonicity of g , we deduce $g(f_1(\rho x)) \leq g(\rho f_1(x))$. Weak scalability of g yields $g(\rho f_1(x)) \leq \rho g(f_1(x))$.

2.(d) Let $x \in \mathbb{R}_+^s$, and let f_1 be an $(A_{0,2})$ -mapping and g be an $(A_{0,1,2,3})$ -mapping. Fix $\rho > 1$. As above, we have $g(f_1(\rho x)) \leq g(\rho f_1(x))$. Then, from scalability of g , it follows that $g(\rho f_1(x)) \ll \rho g(f_1(x))$.

2.(e) Let $x \in \mathbb{R}_+^s$, and let f_1 be an $(A_{0,2,3})$ -mapping, and g be a strictly monotonic $(A_{0,2})$ -mapping. Fix $\rho > 1$. By our assumptions, we have $f_1(\rho x) \ll \rho f_1(x)$, and, from strict monotonicity of g , we have $g(f_1(\rho x)) \ll g(\rho f_1(x))$. Weak scalability of g implies $g(\rho f_1(x)) \leq \rho g(f_1(x))$, and the proof is completed. ■

Appendix C. Proof of Lemma 8

Proof We use the results of Lemma 41 to prove points 1)-7) as follows:

1) Put $f_1(x) = Wx$ and $g(x) = x + b$, and note that f_1 is an $(A_{0,1,2})$ -mapping if W is nonnegative, whereas g is a strictly monotonic $(A_{0,2})$ -mapping for $b \geq 0$. Then, from 2(a)

in Lemma 41, the affine mapping $y_i = W_i x_{i-1} + b_i$ is monotonic, and from 2(d) in Lemma 41, it is also weakly scalable.

2) From point 1) we have that $y_i = W_i x_{i-1} + b_i$ is an $(A_{0,1,2})$ -mapping. To prove scalability, we note that, if $b \gg 0$, then $g(x) = x + b$ is a strictly monotonic $(A_{0,2,3})$ -mapping. The desired assertion now follows from 2(e) in Lemma 41.

3) Monotonicity of T_i follows from 2(a) in Lemma 41 and its weak scalability from 2(d) in Lemma 41.

4) Monotonicity of T_i follows from point 3) above. Scalability of T_i follows from 2(e) in Lemma 41.

5) Monotonicity of T_i follows from point 3) above. Scalability of T_i follows from 2(f) in Lemma 41.

6) Monotonicity and weak scalability of T follows from, respectively, an application of 2(a) and 2(d) in Lemma 41 to consecutive layers of T .

7) Monotonicity of T follows from point 6) above. To prove scalability, verify from 2(e) in Lemma 41 that a subnetwork of T composed of the first i_0 layers of T is scalable. Scalability of T now follows from an application of 2(f) in Lemma 41 to consecutive layers of T , starting with the $i_0 + 1$ -st layer. ■

References

- J. Adler and O. Öktem. Solving ill-posed inverse problems using iterative deep neural networks. *Inverse Problems*, 33(12):124007, 2017.
- A. Ali and F. Yangyu. Automatic modulation classification using deep learning based on sparse autoencoders with nonnegativity constraints. *IEEE Signal Processing Letters*, 24(11):1626–1630, 2017.
- M. A. Arbib and J. J. Bonaiuto. *From Neuron to Cognition via Computational Neuroscience*. MIT Press, 2016.
- B. O. Ayinde and J. M. Zurada. Deep learning of constrained autoencoders for enhanced understanding of data. *IEEE Transactions on Neural Networks and Learning Systems*, 29(9):3969–3979, 2018.
- S. Bai, J. Z. Kolter, and V. Koltun. Deep equilibrium models. *Advances in Neural Information Processing Systems*, 32, 2019.
- S. Bai, V. Koltun, and J. Z. Kolter. Multiscale deep equilibrium models. In H. Larochelle, M. Ranzato, R. Hadsell, M.F. Balcan, and H. Lin, editors, *Advances in Neural Information Processing Systems*, volume 33, pages 5238–5250. Curran Associates, Inc., 2020.
- M. Benning and M. Burger. Modern regularization methods for inverse problems. *Acta Numerica*, 27:1–111, May 2018.
- H. Boche and M. Schubert. Concave and convex interference functions—general characterizations and applications. *IEEE Transactions on Signal Processing*, 56(10):4951–4965, 2008.

- A. D. Burbanks, R. D. Nussbaum, and C. T. Sparrow. Extensions of order-preserving maps on a cone. *Proc. Royal Society of Edinburgh Sect.A*, 133(1):35–59, 2003.
- R. L. G. Cavalcante and S. Stańczak. Weakly standard interference mappings: Existence of fixed points and applications to power control in wireless networks. In *ICASSP 2019 - 2019 IEEE International Conference on Acoustics, Speech and Signal Processing (ICASSP)*, pages 4824–4828, 2019.
- R. L. G. Cavalcante, S. Stańczak, M. Schubert, A. Eisenbläter, and U. Türke. Toward energy-efficient 5G wireless communication technologies. *IEEE Signal Processing Mag.*, 31(6):24–34, Nov. 2014.
- R. L. G. Cavalcante, Y. Shen, and S. Stańczak. Elementary properties of positive concave mappings with applications to network planning and optimization. *IEEE Transactions on Signal Processing*, 64(7):1774–1783, 2016.
- R. L. G. Cavalcante, M. Kasparick, and S. Stańczak. Max-min utility optimization in load coupled interference networks. *IEEE Trans. Wireless Commun.*, 16(2):705–716, Feb. 2017.
- R. L. G. Cavalcante, Q. Liao, and S. Stańczak. Connections between spectral properties of asymptotic mappings and solutions to wireless network problems. *IEEE Transactions on Signal Processing*, 67(10):2747–2760, 2019.
- Renato Luís Garrido Cavalcante and S Stańczak. Spectral radii of asymptotic mappings and the convergence speed of the standard fixed point algorithm. In *2018 IEEE International Conference on Acoustics, Speech and Signal Processing (ICASSP)*, pages 4509–4513. IEEE, 2018.
- Y. Chen, Y. Shi, and B. Zhang. Optimal control via neural networks: a convex approach. In *The International Conference on Learning Representations (ICLR)*, 2019.
- J. Chorowski and J. M. Zurada. Learning understandable neural networks with nonnegative weight constraints. *IEEE Transactions on Neural Networks and Learning Systems*, 26(1):62–69, 2015.
- P. L. Combettes and J.-C. Pesquet. Deep neural network structures solving variational inequalities. *Set-Valued and Variational Analysis*, 28:491–518, September 2020a.
- P. L. Combettes and J.-C. Pesquet. Lipschitz certificates for layered network structures driven by averaged activation operators. *SIAM Journal on Mathematics of Data Science*, 2(2):529–557, June 2020b.
- K. Doya, S. Ishii, A. Pouget, and R. P. N. Rao, editors. *Bayesian Brain: Probabilistic Approaches to Neural Coding*. MIT Press, 2007.
- M. Gabor, T. Piotrowski, and R. L. G. Cavalcante. Positive concave deep equilibrium models. 2024. arXiv:2402.04029 [cs.LG].
- D. Gilton, G. Ongie, and R. Willett. Deep equilibrium architectures for inverse problems in imaging. *IEEE Transactions on Computational Imaging*, 7:1123–1133, 2021.

- I. Goodfellow, Y. Bengio, and A. Courville. *Deep Learning*. The MIT Press, Cambridge, Massachusetts, 2016.
- E. Hosseini-Asl, J. M. Zurada, and O. Nasraoui. Deep learning of part-based representation of data using sparse autoencoders with nonnegativity constraints. *IEEE Transactions on Neural Networks and Learning Systems*, 27(12):2486–2498, 2015.
- Z. Huang, S. Bai, and J. Z. Kolter. In M. Ranzato, A. Beygelzimer, Y. Dauphin, P. S. Liang, and J. Wortman Vaughan, editors, *Advances in Neural Information Processing Systems*, volume 34, pages 9639–9650. Curran Associates, Inc., 2021.
- C. R. Johnson and R. Bru. The spectral radius of a product of nonnegative matrices. *Linear Algebra and its Applications*, 141:227–240, 1990.
- J. Kendall, R. Pantone, K. Manickavasagam, Y. Bengio, and B. Scellier. Training end-to-end analog neural networks with equilibrium propagation. 2020. arXiv:2006.01981 [cs.NE].
- U. Krause. *Positive dynamical systems in discrete time: theory, models, and applications*, volume 62. Walter de Gruyter GmbH & Co KG, 2015.
- Y. A. LeCun, Y. Bengio, and G. Hinton. Deep learning. *Nature*, 521:436–444, 2015.
- D. D. Lee and H. S. Seung. Learning the parts of objects by nonnegative matrix factorization. *Nature*, 401(6755):788–791, 1999.
- A. Lemme, R. F. Reinhart, and J. J. Steil. Online learning and generalization of parts-based image representations by non-negative sparse autoencoders. *Neural Networks*, 33:194–203, 2012.
- B. Lemmens and R. Nussbaum. *Nonlinear Perron-Frobenius Theory*. Cambridge Univ. Press, 2012.
- C. D. Meyer. *Matrix analysis and applied linear algebra*, volume 71. SIAM, 2000.
- T. Miyato, T. Kataoka, M. Koyama, and Y. Yoshida. Spectral normalization for generative adversarial networks. In *International Conference on Learning Representations*, 2018.
- T. D. Nguyen, T. Tran, D. Phung, and S. Venkatesh. Learning parts-based representations with nonnegative restricted Boltzmann machine. In *Asian Conference on Machine Learning*, pages 133–148. PMLR, 2013.
- G. Ongie, A. Jalal, C. A. Metzler, R. G. Baraniuk, A. G. Dimakis, and R. Willett. Deep learning techniques for inverse problems in imaging. *IEEE Journal on Selected Areas in Information Theory*, 1(1):39–56, 2020.
- Y. Oshime. Perron-Frobenius problem for weakly sublinear maps in a Euclidean positive orthant. *Japan Journal of Industrial and Applied Mathematics*, 9(313), 1992.
- M. Paliy, S. Strangio, P. Ruiu, and G. Iannaccone. Assessment of two-dimensional materials-based technology for analog neural networks. *IEEE Journal on Exploratory Solid-State Computational Devices and Circuits*, 7(2):141–149, 2021.

- B. Palsson, J. R. Sveinsson, and M. O. Ulfarsson. Spectral-spatial hyperspectral unmixing using multitask learning. *IEEE Access*, 7:148861–148872, 2019.
- T. Piotrowski and R. L. G. Cavalcante. The fixed point iteration of positive concave mappings converges geometrically if a fixed point exists: Implications to wireless systems. *IEEE Transactions on Signal Processing*, 70:4697–4710, 2022.
- T. A. Poggio and F. Anselmi. *Visual Cortex and Deep Networks*. MIT Press, 2016.
- S. Reich and A. J. Zaslavski. Most continuous and increasing functions on a compact real interval have infinitely many different fixed points. *Journal of Fixed Point Theory and Applications volume*, 25(25), 2023.
- W. Samek, G. Montavon, S. Lapuschkin, C. J. Anders, and K.-R. Müller. Explaining deep neural networks and beyond: A review of methods and applications. *Proceedings of the IEEE*, 109(3):247–278, 2021.
- M. Schubert and H. Boche. *Interference Calculus - A General Framework for Interference Management and Network Utility Optimization*. Springer, Berlin, 2011.
- M. Shashanka, B. Raj, and P. Smaragdis. Probabilistic latent variable models as nonnegative factorizations. *Computational Intelligence and Neuroscience*, 2008(Article ID 947438), 2008.
- S. Shindoh. The structures of SINR regions for standard interference mappings. In *2019 58th Annual Conference of the Society of Instrument and Control Engineers of Japan (SICE)*, pages 1280–1285. IEEE, 2019.
- S. Shindoh. Some properties of SINR regions for standard interference mappings. *SICE Journal of Control, Measurement, and System Integration*, 13(3):50–56, 2020.
- Y. Su, A. Marinoni, J. Li, J. Plaza, and P. Gamba. Stacked nonnegative sparse autoencoders for robust hyperspectral unmixing. *IEEE Geoscience and Remote Sensing Letters*, 15(9):1427–1431, 2018.
- R. Tsuchida and C. S. Ong. Deep equilibrium models as estimators for continuous latent variables. In Francisco Ruiz, Jennifer Dy, and Jan-Willem van de Meent, editors, *Proceedings of The 26th International Conference on Artificial Intelligence and Statistics*, volume 206 of *Proceedings of Machine Learning Research*, pages 1646–1671. PMLR, 2023.
- M. Woodford. Effective demand failures and the limits of monetary stabilization policy. *American Economic Review*, 112(5):1475–1521, May 2022.
- I. Yamada, M. Yukawa, and M. Yamagishi. Minimizing the Moreau envelope of nonsmooth convex functions over the fixed point set of certain quasi-nonexpansive mappings. In H. H. Bauschke, R. S. Burachik, P. L. Combettes, V. Elser, D. R. Luke, and H. Wolkowicz, editors, *Fixed-Point Algorithms for Inverse Problems in Science and Engineering*, pages 345–390, New York, NY, 2011. Springer New York.

- L. You and D. Yuan. A note on decoding order in user grouping and power optimization for multi-cell NOMA with load coupling. *IEEE Transactions on Wireless Communications*, 2020.
- S. Yu, M. Drton, and A. Shojaie. Generalized score matching for non-negative data. *Journal of Machine Learning Research*, 20(76):1–70, 2019.
- M. Zhou, Y. Cong, and B. Chen. Augmentable gamma belief networks. *Journal of Machine Learning Research*, 17(163):1–44, 2016.